Saguenay, le 19 août 2020

Madame Joannie Martin
Gestionnaire de projet, Bureau régional du Québec
Agence d'évaluation d'impact du Canada
1550, avenue d'Estimauville
Québec (Québec) G1J 0C1

Objet : Projet Énergie Saguenay – Complexe de liquéfaction de gaz naturel à Saguenay.
Dépôt de l'addenda 2 du document-réponses en complément à la première demande d'information sur l'étude d'impact environnemental et révision de la portée du projet en lien avec la navigation (No dossier 005543) : ACEE-78 Risques sismiques

Madame Martin,

Vous trouverez annexé à cette lettre, un rapport d'évaluation des aléas sismiques spécifiques au site réalisé par la firme Nanometrics inc. en réponse à la question ACEE-78. Puisque le rapport est rédigé en anglais, vous trouverez ci-dessous une traduction du sommaire exécutif.

Une évaluation probabiliste des aléas sismiques (PSHA) propre au site a été menée pour un complexe de liquéfaction de gaz naturel proposé près de Saguenay, au Québec. L'évaluation est réalisée par Nanometrics en collaboration avec le Dr Gail Atkinson, qui a agi en tant que conseiller technique pour l'étude. Ce rapport décrit la méthodologie, les hypothèses et les résultats.

L'objectif principal était de déterminer les spectres d'aléa uniformes horizontaux et verticaux pour une condition de roche dure (site de classe A), pour des périodes de retour de 475, 975 et 2 475 ans. Les zones de sources sismiques sont définies pour modéliser le taux d'activité, la distribution spatiale et la magnitude maximale dans un rayon de moins de 500 km du site. L'approche du zonage de la source consiste à commencer avec les zones et les taux de source régionaux déterminés par la Commission géologique du Canada (CGC), et à explorer les modifications qui pourraient être nécessaires pour l'adaptation des modèles au site. Une série de modèles de mouvement du sol qui caractérisent les mouvements sismiques potentiels et l'incertitude épistémique associée pour la condition du site de référence est développée sur la base des modèles prédictifs récemment mis à jour et de l'approche « scaled-backbone ».

L'aléa sismique obtenu pour le site à l'étude est supérieur aux valeurs publiées par la CGC basées sur le modèle de risque régional de 5e génération pour toutes les périodes de retour d'intérêt. Ceci est principalement attribué à (i) l'utilisation de modèles de mouvement du sol mis à jour dans cette étude et (ii) la mise en œuvre de la méthode de lissage de sismicité (« smoothed seismicity » qui résulte en une

concentration de la sismicité potentielle autour des zones plus proches du site où les failles sont concentrées et la sismicité passée a été observée.

L'analyse de désagrégation des aléas indique que, pour la période de retour de 475 ans, les séismes de magnitude modérée dans la région de Charlevoix sont dominants. Pour les périodes de retour de 975 et 2 475 ans, les séismes de magnitude modérée dans la région du Saguenay commencent à dominer les périodes courtes à intermédiaires, alors que les longues périodes sont contrôlées par des séismes de grande magnitude dans la région de Charlevoix.

Espérant le tout conforme à vos attentes, nous vous prions d'agréer nos salutations distinguées.

<Original signé par>

_____
Sylvain Ménard
Directeur Environnement

SM/

p. j. Site-Specific Seismic Hazard Assessment for a Proposed LNG Facility near Saguenay, Québec: Technical Report

c.c. : Nathalie Fortin, Directrice de service provincial - Gestion environnementale

345, rue des Saguenéens, bureau 210
Chicoutimi, Québec G7H 6K9
energiesaguenay.com

Site-Specific Seismic Hazard Assessment for a Proposed LNG Facility near Saguenay, Québec

Technical Report

Prepared for

GNL QUÉBEC

August 2020

DISCLAIMER

ATTENTION: PLEASE READ CAREFULLY

The information prepared by Nanometrics Inc. ("Nanometrics") and contained in this document is intended to report and provide insights for the full use, as required, of the recipient(s) of this document. Recipient(s) acknowledge that, if applicable, the overall outputs contained in this document are estimates by their nature, as they are dependent upon measurements and mathematical models with varying levels of inherent uncertainty and assumptions that are typical of empirical and statistical analysis. The findings in this document should be assessed as a whole and any attempt to rely on partial analysis or summary descriptions in this document could lead to undue emphasis on particular factors or inaccurate conclusions.

The information in this document is provided with the understanding that this document is intended for use as part of a wider scope of work that may be provided by Nanometrics and Nanometrics is not providing any professional advice or recommending any one course of action based on the contents of this document.

Nanometrics endeavours to provide accurate and reliable information and insights. This document has been provided in good faith based on data collected by Nanometrics which was available at the time the document was generated and which is dependent on various factors including, but not limited to, the number, geographical distribution and/or, if applicable, the performance of commissioned stations which may be affected by factors outside of the control of Nanometrics. Without limiting the foregoing, Nanometrics Inc. specifically disclaims any responsibility if this document is inaccurate, incomplete or misleading at the time of distribution.

All information in this document is provided "as is", without warranty of any kind, express or implied, including, but not limited to any warranties of merchantability, merchantable quality or fitness for a particular purpose. In no event will Nanometrics, or its partners, suppliers, employees or agents, be liable to the recipient(s) or anyone else for any loss, damage, cost or expense of any kind, including any consequential, special or similar damages, arising in connection with results obtained from the use of this information, any decision made or action taken in reliance on this document or any information contained in this document.

Table of Contents

1. Executive Summary

A site-specific probabilistic seismic hazard assessment (PSHA) is conducted for a proposed liquid natural gas (LNG) processing facility site near Saguenay, Québec. The assessment is performed by Nanometrics in collaboration with Dr. Gail Atkinson, who acted as a technical advisor for the study. This report describes the methodology, assumptions and findings for the conducted PSHA study.

The primary objective is to determine the horizontal and vertical uniform hazard spectra for a hard rock condition (Site Class A), for return periods of 475, 975 and 2475 years. Seismic source zones are defined to model the activity rate, spatial distribution, and maximum magnitude within 500 km of the site. The approach to source zonation is to begin with the regional source zones and rates as determined by the Geological Survey of Canada (GSC), and explore modifications that may be required to make the models suitable for application to the site. A suite of ground motion models that characterize the potential earthquake motions and associated epistemic uncertainty for the reference site condition is developed based on the recently updated predictive models and the scaled-backbone approach.

The ground-motion hazard at the target site is greater than the GSC's published values based on the regional 5th generation hazard model for all return periods of interest. This is primarily attributed to (i) the use of updated ground motion models in this study and (ii) the implementation of smoothed seismicity method which resulted in concentration of potential seismicity around the areas closer to the site where faults are concentrated and past seismicity has been observed.

Hazard disaggregation analysis indicates that for the 475-year return period the hazard is controlled by moderate magnitude earthquakes in the Charlevoix area. For the 975- and 2475-year return periods, moderate magnitude earthquakes within the Saguenay region begin to dominate short-to-intermediate periods, whereas long periods are controlled by large magnitude earthquakes in the Charlevoix area.

2. Introduction

A site-specific seismic hazard assessment is conducted as input for the design of a proposed LNG facility within the Saguenay Fjord (Figure 1). In accordance with the standard CAN/CSA-Z276-18, uniform response spectra (UHS) and peak ground accelerations (PGA) are determined for three return periods of interest: 475, 975 and 2475 years. Hazard assessment is performed for a generic hard rock condition (Site Class A).

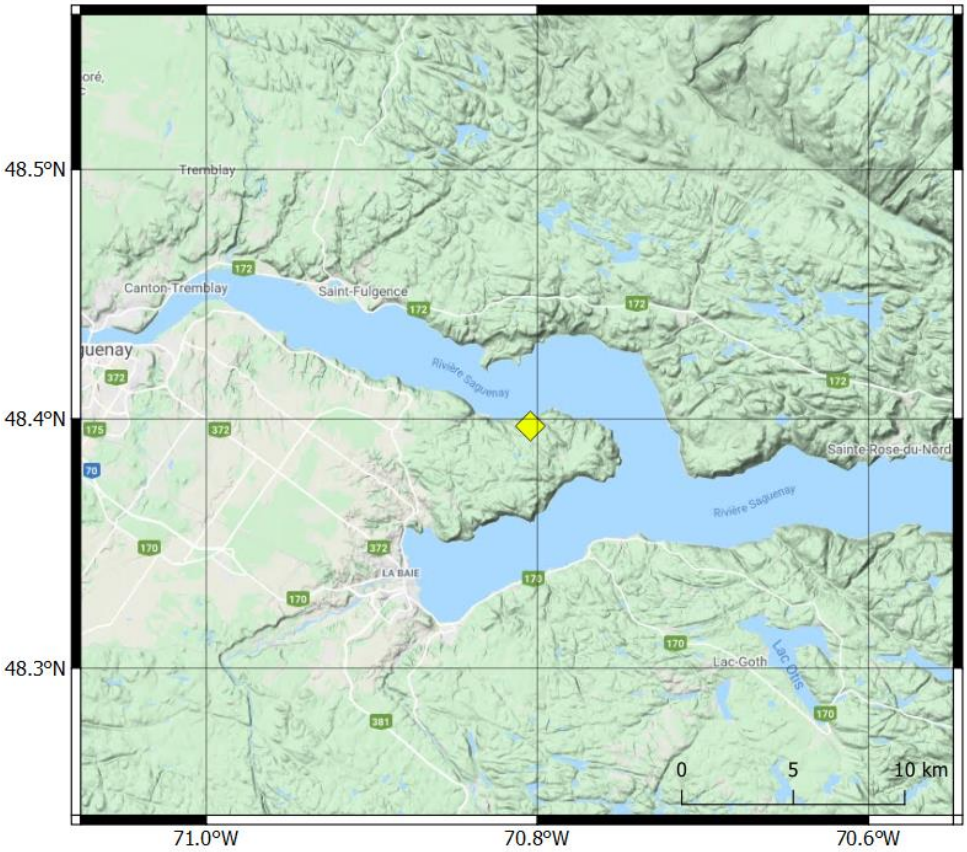

Figure 1. Location of the proposed LNG facility (yellow diamond) within the Saguenay Fjord

Seismic hazard is estimated using the probabilistic Cornell-McGuire method that accounts for the uncertainty in location and magnitude of potential future earthquakes at local and regional sources. Earthquake occurrence is linked to the resultant ground motions at the target site using ground motion models (GMMs), which also account for uncertainty and variability in earthquake motions. The probabilistic method forms the basis for the seismic hazard maps in Canadian building codes. This assessment represents a refinement of the 5th generation hazard model (Halchuk et al., 2015) developed by the Geological Survey of Canada (GSC) with focus on the potential seismicity and their ground motions in the site vicinity.

Site-specific hazard analysis is performed to determine hard rock UHS and PGA for return periods of interest. Vertical-component ground-motion hazard is estimated from the horizontal motions using published horizontal-to-vertical (H/V) ratios. This study showed that the ground-

motion hazard at the target site is greater than the GSC's published values based on the regional 5th generation hazard model for all return periods of interest. This is primarily attributed to the use of updated ground motion models in this study as well as the implementation of smoothed seismicity method which resulted in concentration of potential seismicity around the areas closer to the site where faults are concentrated and past seismicity has been observed.

The seismic hazard is disaggregated to identify the magnitudes and distances that contribute most to the hazard at the target site. It is found that 475-year hazard is dominated by earthquakes in Charlevoix area with magnitudes $6.0 < M < 6.5$. For the 975-year return period, contributions for short spectral periods ($T < 0.1$ s) become apparent at local distances (~30 km) with moderate magnitude earthquakes ($5.5 < M < 6.0$). At intermediate and long periods ($T \geq 0.1$ s) the hazard controlled by earthquakes of $6.0 < M < 7.0$ from Charlevoix area. For the 2475-year return period, hazard at short and intermediate periods ($T < 1$ s) is dominated by $6.0 < M < 6.5$ earthquakes in Saguenay area, whereas long period contributions come from $7.0 < M < 7.5$ Charlevoix area.

3. Methodology

Seismic hazard analyses in Eastern Canada are based on probabilistic concepts which allow incorporation of both geologic interpretations of seismic potential and statistical data regarding the locations and sizes of past earthquakes. The Cornell-McGuire method (Cornell, 1968; McGuire, 1976, 1977, 2004) has proven particularly well-suited to calculate expected ground motions for a wide range of seismic hazard environments. It forms the basis for the seismic hazard maps in the National Building Code of Canada since 1985, and is the usual basis for seismic hazard evaluations of important engineered structures.

With probabilistic seismic hazard assessment (PSHA), ground motions that may be produced by future earthquakes at a target site can be estimated for a desired annual probability of exceedance, considering uncertainties in their location, magnitude and ground motion. Uncertainties involved in PSHA are grouped into two categories: epistemic and aleatory uncertainty. The former refers to the model uncertainty due to incomplete knowledge regarding the processes governing earthquake occurrence and ground motion generation. It implies a spread of possible results about those that might be considered a best estimate. This type of uncertainty is typically considered using a logic tree framework where alternative source and ground motion models are represented with associated weighting. The aleatory uncertainty, on the other hand, refers to the random uncertainty due to the physical variability of earthquake processes. It is incorporated directly into the probabilistic analysis as part of the integral sum of possible earthquake scenarios.

In this study, seismic hazard is determined based on the probabilistic method. The spatial distribution of earthquakes is described by defining seismic source zones (areas which may contain groups of faults) on the basis of seismicity and seismotectonic interpretations. The 5th generation seismic source model of GSC (Halchuk et al., 2015) is examined to determine whether it accurately represents the potential seismicity at the site vicinity. The frequency of earthquake occurrence for each source zone is described by a magnitude-recurrence (MR) relationship, truncated at a maximum magnitude, Mx. The source zones and associated MR models of GSC are checked for applicability based on the observed seismicity patterns using an up-to-date earthquake catalog. Seismic sources within 500 km of the site are considered in the analysis. A literature survey is conducted to understand the seismicity potential of known faults near the target site.

Earthquake ground-motion models (GMMs) provide the link between the occurrence of earthquakes of various magnitudes and the resulting ground motion levels at the site. Two alternative suites of GMMs are considered in the hazard analysis. Both GMM suites are developed using the scaled-backbone approach (Atkinson et al., 2014). The first suite is derived from the 17 seed GMMs that were developed for Central and Eastern North America in the Next Generation Attenuation - East (NGA-East; Goulet et al., 2018) project. The second GMM suite is constructed based on the predictive model of Atkinson et al. (2015), which was developed for earthquakes in southern Ontario and western Quebec. The epistemic uncertainty in median predictions is modeled based on a logic-tree approach, where the distribution of potential

median predictions is approximated using a lower, central and upper model. For each GMM suite, the central backbone model is defined, which is then scaled to define the corresponding lower and upper branch models. Aleatory variability of ground motions is treated independently from the specification of the median ground motions and associated epistemic uncertainty. The available data are insufficient to model aleatory variability with confidence. Consistent with the 5^{th} generation hazard model, the representative aleatory variability values as proposed by Atkinson and Adams (2013) are used in this study.

The probability of exceeding a specified level of ground motion at the site is calculated by summing up the hazard contributions over all magnitudes and distances, including sources within 500 km of the site. The open-source EqHaz software package (Assatourians and Atkinson, 2013; 2019) that is based on Monte Carlo simulation approach is used for the hazard analysis. The EqHaz software consists of three components:

- EqHaz1 generates synthetic earthquake catalogs by randomly drawing sets of recurrence parameters using a source-model logic tree and associated weights, in order account for epistemic uncertainties in source modeling. This is repeated for each source zone and realization. Event locations are assigned based on the choice of uniform or smoothed seismicity methods (discussed later).
- EqHaz2 generates synthetic ground motion catalogs using the earthquake catalogs generated by EqHaz1. It determines ground motions that would be experienced at a target site for each synthetic event based on the probabilistic approach. Ground motion amplitudes are randomly sampled using a GMM logic tree and aleatory variabilities. EqHaz2 calculates hazard curves and the uniform hazard spectra (UHS) by summing up ground-motion hazard contributions from all magnitudes and distances.
- Hazard disaggregations are performed using EqHaz3, where the relative hazard contributions at magnitude – distance pairs are extracted.

In this study, hazard analysis is performed for 12 oscillator periods of interest between 0.01 s ≤ T ≤ 10 s, to calculate UHS for each annual probability of interest (1/475, 1/975 and 1/2475). Hazard values for peak ground acceleration (PGA) are also determined for the same annual probabilities.

4. Regional Tectonic Setting

The project site is located in an intraplate tectonic setting where Iapetan rift structures occur. These structures were created during the rifting and opening of the Iapetus Ocean in the late Proterozoic, 700–600 Ma (Kumarapeli, 1985; Mazzotti et al., 2005). This major episode of extension corresponds to the formation of large-scale systems of normal faults along the rifted margin and associated aulacogens across most of Eastern North America. The Appalachian nappes were thrust over the North America craton during the close of the Iapetus Ocean in mid to late Paleozoic, possibly as late as Permian approximately 250 Ma (Williams, 1979; Faure et al., 1996). The last phase of significant tectonic activity in the St. Lawrence area was during the Jurassic rifting and opening of the North Atlantic Ocean, which marks the reactivation of Iapetan normal faults (Lemieux et al., 2003).

The St. Lawrence Rift System (SLRS) is characterized by NE-SW trending faults and establishes the boundary between the Grenville Province of the Canadian Shield to the northwest and the St. Lawrence Lowlands to the southeast (Lamontagne and Ranalli, 2014). The grabens of Ottawa–Bonnechere and Saguenay River intersect the SLRS and are both interpreted as Iapetan failed arms (Kumarapeli, 1985; Tremblay and Roden-Tice, 2011) (PEM and SAG zones of Figure 3). Faults related to the Ottawa–Bonnechere and Saguenay grabens trend mostly WNW–ESE.

Rifting of the Saguenay region was dated concurrent with the breakup of Pangea and the onset of continental rifting 200-250 Ma ago (Tremblay et al., 2013). The Saguenay fault system is represented by two major subparallel normal faults, the Sainte-Marguerite River fault to the north, and the Lac- Kénogami fault to the south (Figure 2). These two faults bound the Saguenay River and extend laterally for several tens of kilometers. At present, there are no clear indications that pre-existing structures of the Grenvillian basement have controlled the development of either the St. Lawrence or Saguenay fault systems (Tremblay et al., 2013).

The SLRS and its associated failed Iapetan arms has hosted many of the large (M>5) earthquakes in Eastern Canada (Lamontagne et al., 2008). The associated seismicity is notably clustered in three zones: (i) along the Ottawa River (MNT, PEM and KIP zones of Figure 3), (ii) Charlevoix, a repetitive source of large earthquakes and a continuous source of small earthquakes (CHV zone of Figure 3), and (iii) the lower St. Lawrence, a diffuse zone of mostly small earthquakes (BSL zones of Figure 3). Most earthquakes in these zones are thrust events with no known surface ruptures, occurring at depths of 5 to 25 km within the Grenville cratonic basement, primarily through the reactivation of the existing faults in the current compressional stress regime (Adams and Basham, 1991; Lamontagne and Ranalli, 2014). The largest eastern Canadian earthquake in the last 50 years, the 1988 Mw5.9 (where Mw is moment magnitude) Saguenay earthquake, occurred on the margin of the Saguenay rift (SAG zone of Figure 3) 40 km to the south west of the study site. Prior to the 1988 Saguenay earthquake sequence, the area was considered seismically inactive (Du Berger, 1991).

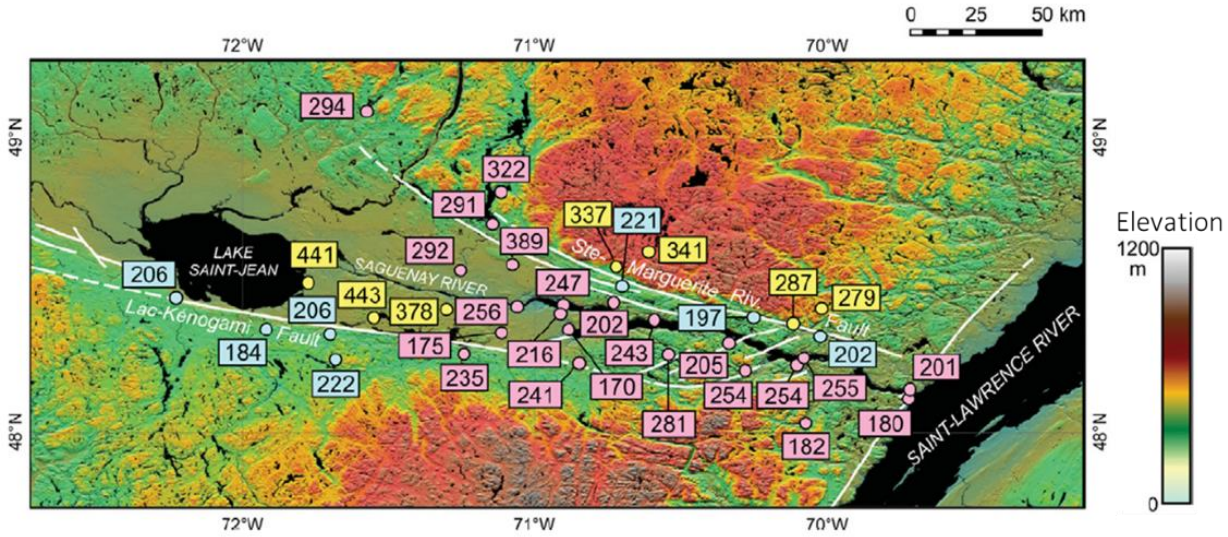

Figure 2. Age (in Ma) distribution for the Saguenay River fault system based on apatite fission-track dating (modified from Tremblay et al., 2013). Blue boxes are for footwall samples and yellow boxes are for hanging-wall samples of the Lac-Kénogami and Sainte-Marguerite River faults. Pink boxes are for the Saguenay River valley (north and south shores).

The causes of earthquakes in Eastern Canada are not well understood. The superposition of the regional stress field and the relatively modest post-glacial rebound stresses are likely to play a role in earthquake occurrence in the area. It is argued that the localized seismic zones may simply be an artifact of limited time period of seismic data collection within a transient system. Over time, seismicity may be more evenly distributed along the paleotectonic structure network, but with only small portions active over short intervals (Braid, 2010; Swafford and Stein, 2007). However, the presence of pre-existing faults related to the SLRS does not explain all the features of the known seismicity (such as the seismicity north of the Ottawa River in western Quebec, the GAT zone on Figure 3). It is proposed that other factors such as local weaknesses and stress conditions, in addition to the Iapetan rift faults, may lead to the earthquakes concentrated in certain areas along the SLRS (Tuttle and Atkinson, 2010; Lamontagne and Ranalli, 2014).

Located about 100 km downriver from Saguenay, the Charlevoix seismic zone is the most active area in the region, with numerous small to medium earthquakes as well as five M>6 events in the last 350 years (Mazzotti et al., 2005). In contrast, the area between Quebec City and Montreal, which both lie along the same rift system, show less seismic activity. The elevated seismic activity in Charlevoix region has been attributed at least in part to a meteorite impact (~350 Ma) in the southern part of the area, which contributed additional complexity by creating a ~60 km diameter system of concentric faults and fractures (Rondot, 1968; Lemieux et al., 2003). Lamontagne (1987) showed that microearthquakes within the impact structure have more varied mechanisms than those outside it, due to the extra structural complexity caused by the impact. According to Baird et al. (2009, 2010), the weakening of the rift faults produces a stress increase in the region of the crater bounded by faults, leading to low-magnitude events within the crater and large events outside it.

Another possibility for the reactivation of local faults is the role of subcrustal processes. For example, the NW-SE trending band of seismicity in western Quebec (north of the Ottawa River, GAT zone on Figure 3) could be related to an extension of the New England Seamount Chain track or the passage of this region over the Great Meteor hotspot between 140 Ma and 120 Ma (Sykes, 1978; Crough, 1981; Adams and Basham, 1989). Crough (1981) demonstrated that the passage of the hot spot caused a local uplift of the shield, resulting in erosion of at least 1 km at Montreal and perhaps 6 to 7 km in New England. Although the hot spot may have been less well developed when western Quebec passed over it, the Precambrian crust in western Quebec may have been thermally stressed and fractured by differential uplift during the passage of the hot spot (Adams and Basham, 1991). This geologically recent weakening of the North American craton may have localized the release of seismic energy today.

5. Seismic Source Characterization

The first step in the seismic hazard assessment is the characterization of seismogenic sources in the area of interest. In this study, seismic sources within 500 km of the site are considered for the hazard assessment. An up-to-date earthquake catalog is compiled from available seismological databases and used to check and refine the zonation and magnitude-recurrence (MR) relations of the 5th generation source model.

A literature survey is conducted to understand the seismicity potential of known faults near the target site. The aim of the literature survey is to determine whether there are identified faults that represent an additional hazard that is not already implicitly considered in the source zone models. This could include faults with significant geologic slip, or that show some indication that they may concentrate seismicity relative to that of the surrounding area. The local treatment of sources, including potential faults, is reported in Section 5.4.

5.1. Base Source Model

The 5th generation seismic source model developed by the GSC (Halchuk et al., 2015) is adopted as a base model in this study[1]. In Eastern Canada, it consists of three alternative interpretations of potential seismicity: a historical model (H2), a regional seismotectonic model (R2) and a hybrid model (HY). The H2 model (Figure 3) is composed of conventional areal sources defined on the basis of historical seismicity clusters under the assumption that these clusters will continue to produce earthquakes. This model comprises a number of relatively small source zones together with a few large background zones. Though the zone boundaries are largely chosen to enclose seismicity clusters, there is also some account taken of broad regional geological features such as the Iapetan rifted margin (sources that follow the St. Lawrence River). The important zones of historical activity for this project are:

- Saguenay (SAG) Seismicity Zone: It captures the seismicity in Saguenay region that extends 121 km to the north west of the site, and 71 km to the south east of the site where it borders the Charlevoix zone. The 1988 Mw5.9 Saguenay earthquake, which caused damage in the area, is the largest historic event recorded in this zone.
- Charlevoix (CHV) Seismicity Zone: It includes the seismicity between Charlevoix County on the north shore and Kamouraska County on the south shore. This is the most seismically active region in Eastern Canada. Historically, the CHV zone has been subject to five large earthquakes: ~M7.5 in 1663[2] (Ebel, 2011), ~M6 in 1791, ~M6 in 1860, ~M6.5 in 1870 and M6.2 in 1925 and hundreds of smaller events (Halchuk et al., 2015).

[1] The 6th generation hazard model was in preparation at the time of this study. It uses most of the same seismic sources as in the 5th generation model with some changes to those in Western Canada. The earthquake catalog and MR relations for source zones in Eastern Canada were kept the same in the 6th generation source model (Adams et al., 2019).

[2] Based on geological investigations, Locat et al. (2003, 2009, 2011) proposed that this earthquake may occurred in SAG zone (discussed later).

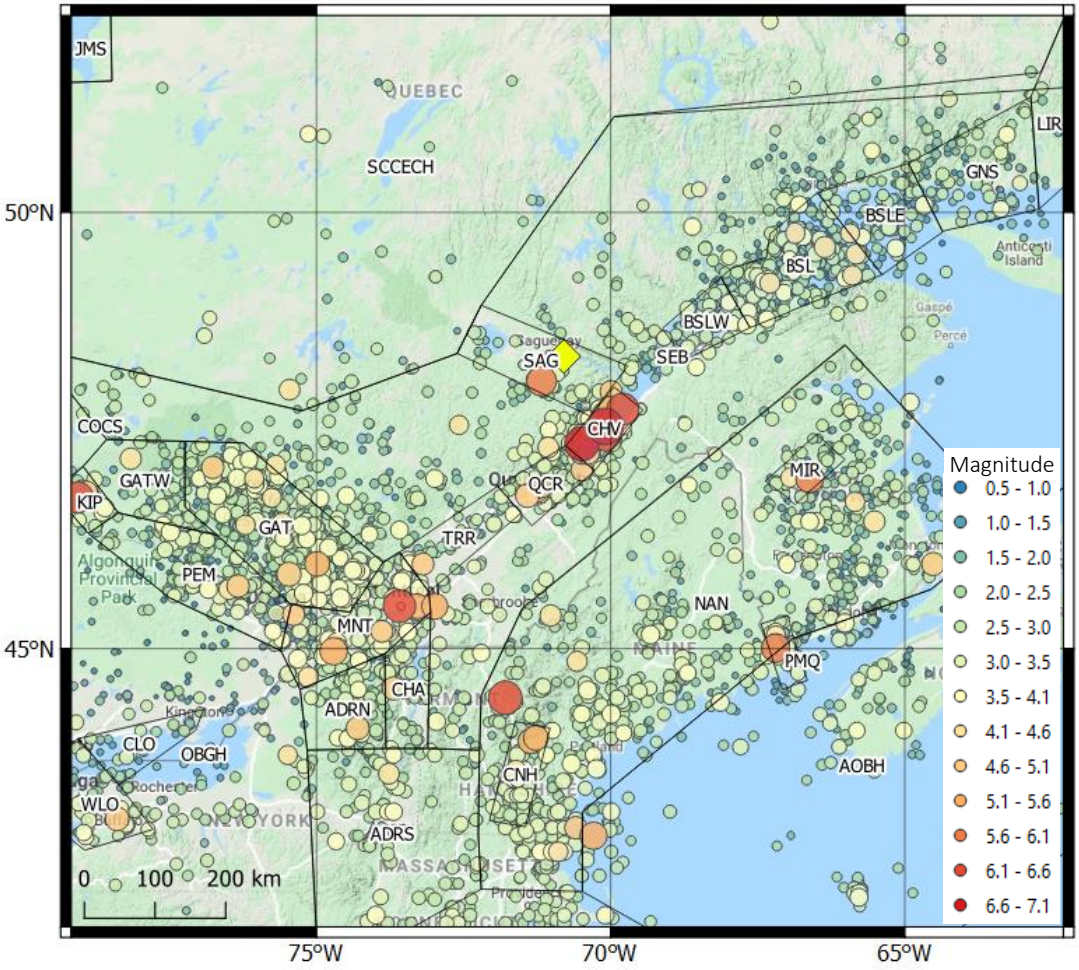

Figure 3. Seismic source zonation for H2 model. Seismicity through the end of 2019 (after the completeness screening) is also shown. Diamond symbol indicates the project site.

The R2 model (Figure 4) follows broad regional seismotectonic units, implicitly smoothing the activity of clusters across larger regional zones. The implicit assumption is that clusters within the seismotectonic zones may migrate over long time scales (many hundreds to thousands of years), with currently-active clusters dying out, and new clusters initiating elsewhere. Seismic reflection profiles in the Charlevoix area fail to show significant accumulated slip across Quaternary deposits, suggesting that significant seismic activity in the Charlevoix seismic zone is relatively young, perhaps only a few thousand years (Lamontagne, 1999). Due to the spatial association of known seismicity with the Iapetan rift structures and the long return periods of major earthquakes in Eastern North America (ENA), it is likely that historical seismicity has not revealed the locations of all seismogenic structures. For these reasons, it has been postulated that future large earthquakes (M>6) may be equally likely anywhere within broad source zones that encompass tectonically-similar geologic structures (Adams and Basham, 1989; Johnston et al. 1994; Swafford and Stein 2007). On the other hand, paleoseismic investigations suggest that for the last ~10,000 years the rate of large earthquakes appears to have been much higher in the Charlevoix seismic zone than in adjacent areas of the St. Lawrence, and thus the presence of

Iapetan rift faults that underlie the St. Lawrence Valley of southeastern Canada may not be entirely indicative of potential earthquake hazard (Tuttle and Atkinson, 2010).

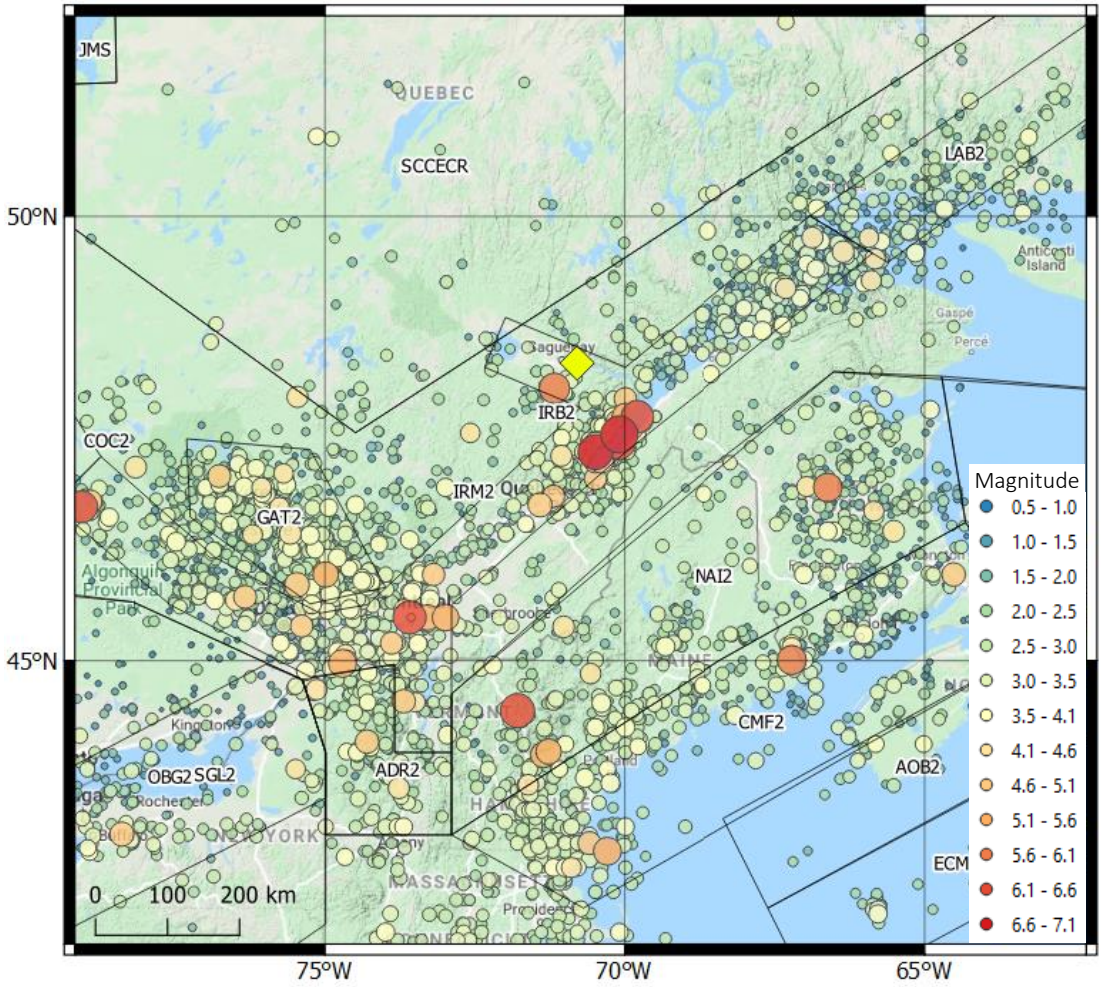

Figure 4. Seismic source zonation for R2 model. Seismicity through the end of 2019 (after the completeness screening) is also shown. Diamond symbol indicates the project site.

The HY model (Figure 5) is a hybrid that takes elements from both the historical and tectonic models. It is argued that historic large events in Eastern Canada (e.g., 1663 ~M7 Charlevoix earthquake) may be considered as characteristic mainshocks, which induced clusters of seismicity in the vicinity that may last hundreds of years, followed by a period of quiescence that might last thousands of years (Adams and Basham, 1989; Crone et al., 2003; Stein et al., 2009). This conceptual model implies that large earthquakes (M > 6.5) cannot be predicted simply on the basis of a relatively short earthquake history and can occur anywhere along the SLRS with equal probability as characteristic events, whereas small-to-moderate earthquakes (M < 6.5) occur according to recently observed seismicity in segmented zones, with significant departures from the observed seismic rates being unlikely in the near future (Atkinson and Goda, 2011). In practice the HY model is implemented by using the zones of historical seismicity clusters to model the recurrence parameters for earthquakes up to M6.8. Broader overlying regional

seismotectonic sources are used to model recurrence parameters events of M>6.8, up to the same maximum magnitudes as for the H2 model. The HY model uses all of the sources in the H2 model (for earthquakes up to M6.8) together with large seismotectonic sources, which are intended to capture the occurrence of rare, large earthquakes. To avoid double counting, the Mx for most of the H2 zones was capped at M6.8. However, because the large seismotectonic sources do not cover the entire areal extent of the H2 zones the Mx in nonoverlapped zones were retained at their original H2 values.

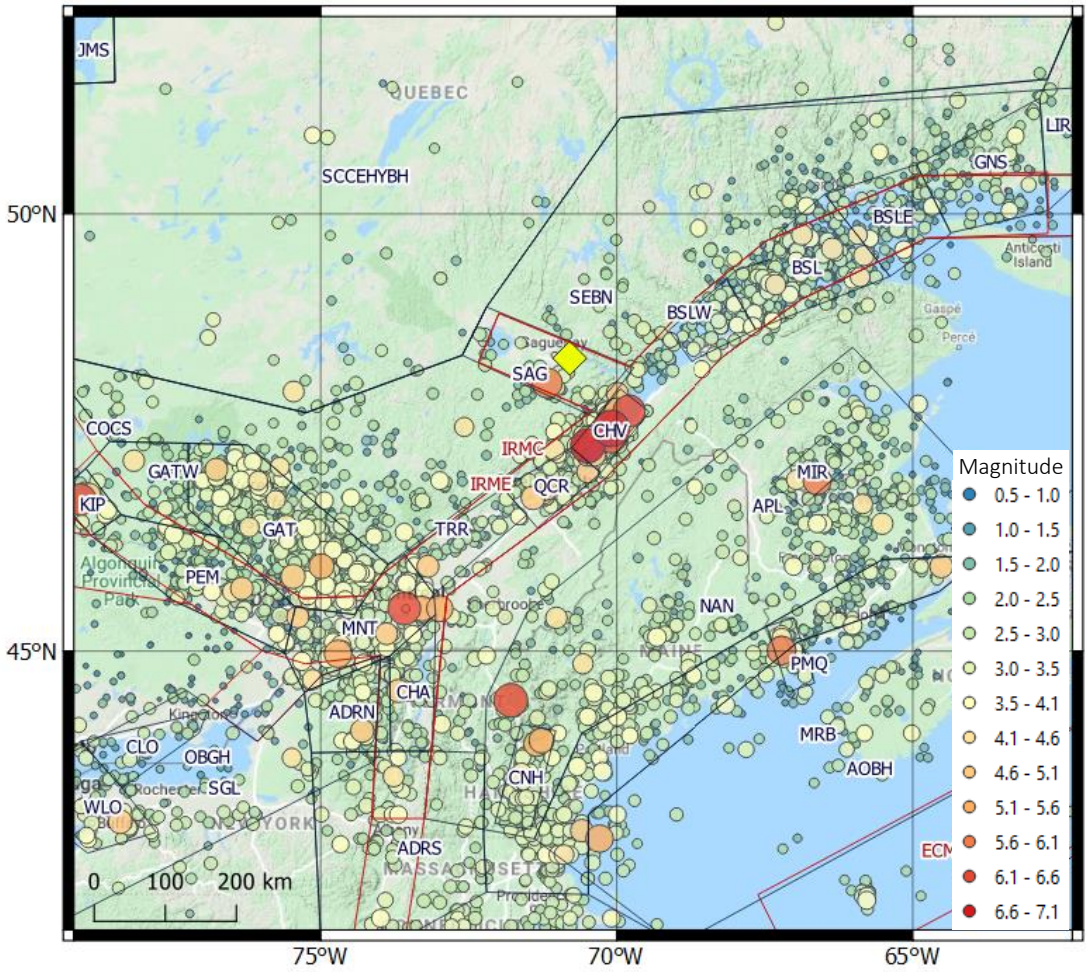

Figure 5. Seismic source zonation for HY model. Seismicity through the end of 2019 (after the completeness screening) is also shown. Diamond symbol indicates the project site.

5.2. Regional Earthquake Catalogue

The adopted base source model relies on the Seismic Hazard Earthquake Epicentre File (SHEEF) compiled by Halchuk et al. (2015). The SHEEF catalogue includes all known seismic events with a magnitude of M≥2.5 through the end of 2010. In this study, it is updated with new events reported by GSC and the USGS from the beginning of 2011 to the beginning of June, 2020. The

reported magnitudes are converted to moment magnitude (Mw) following the same approach of Halchuk et al. (2015) in order to maintain consistency with the SHEEF catalogue. Events that are smaller than the minimum magnitude of completeness, as defined by Adams and Halchuk (2003), are excluded in the assessment of recurrence rates.

In many regions, it is common to decluster a catalogue to remove aftershocks before conducting the PSHA, in order to satisfy the stationarity assumptions of the Poisson distribution. This has not been the common practice in most regions of Canada, particularly in eastern Canada. There are several reasons for this. One is specific to earthquake recurrence models in this region. Aftershock sequences for large intraplate earthquakes may continue for long durations (hundreds to thousands of years) (Stein and Liu, 2009; Leonard et al., 2014) rendering traditional declustering techniques unsuitable. For example, some researchers posit that the ongoing activity in CHV zone is part of a long aftershock sequence of the 1663 event (Ebel, 1984; Adams and Basham, 1991). Under this logic, most seismicity (and hazard) would be removed by declustering, which would clearly not be appropriate, as seismicity is ongoing. Furthermore, recent work suggests that declustering algorithms can lead to biased b-values (Llenos and Michael, 2020), and that the practice of declustering may be unjustified in many cases. Moreover, some argue that the events that occur are part of the hazard, as they contribute to the overall moment budget for the region. Finally, sensitivity tests in selected regions of Canada (Adams, pers. comm.) suggest that, if one uses a manual procedure to remove suspected aftershocks, this does not significantly impact the calculated hazard (in comparison to leaving the aftershocks in). Therefore, the GSC has not removed aftershocks in development of either the 5th or 6th generation hazard models (with rare exceptions), and that practice is followed in this study. Therefore, the event catalogue is not declustered.

5.3. Magnitude Recurrence Relations for Important Source Zones

The zonation and magnitude-recurrence (MR) relations of the base source model are examined using the updated event catalogue, with focus given to the hazard-significant zones. Figure 6 shows a comparison of the spatial distribution of earthquakes and the H2 source model for the area within ~200 km of the site. The GSC's choices in terms of source zone boundaries for the H2 model appears to be appropriate on a regional scale, with seismicity clustering largely within the defined zone boundaries.

GSC adopted MR relations of the 5th generation source model for use in the 6th generation model (Adams et al., 2019). For a given source zone, the MR relation is characterized in terms of alternative combinations of activity rate (a-value), slope (b-value) and maximum magnitude (Mx) in order to account for the epistemic uncertainty in the rate of earthquakes. GSC provides three alternative values (best, lower and upper) for a-b pairs and Mx, corresponding to a total of nine MR relations for each source zone. The a- and b-values were generally determined based on the maximum likelihood statistics together with uncertainty bounds on the best-fit relation (Adams et al.,2015). In some cases, the best b-values were defined based on the regional average values

(e.g., QCR) or the rates of large historical events (e.g., CHV and SAG). The maximum magnitudes were identified by considering the largest events observed in tectonically-analogous regions worldwide, largest historical event in the region and GPS strain rates (Mazzotti et al., 2005; Adams et al.,2015).

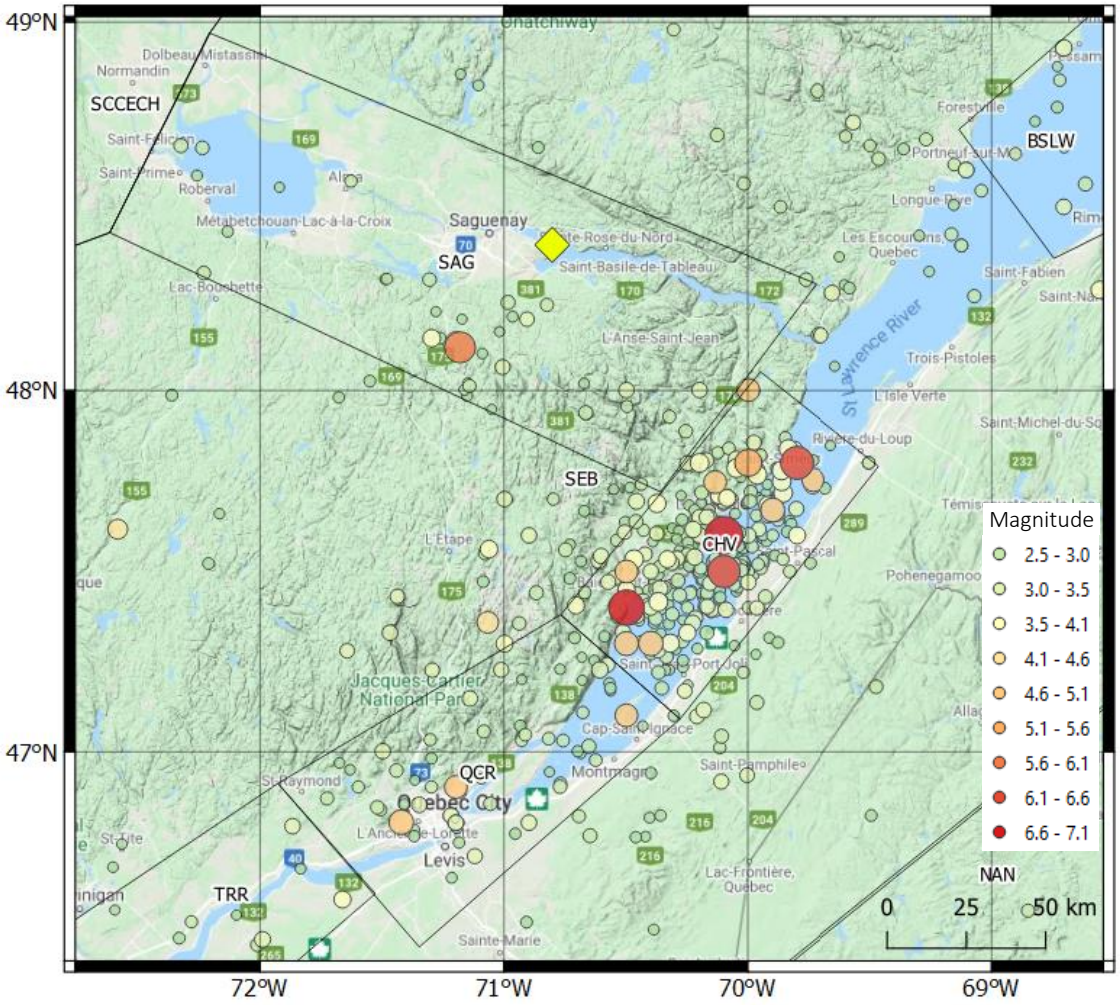

Figure 6. Earthquakes of Mw≥2.5 through the end of May, 2020 (after the completeness screening) and the H2 source model for zones within ~200 km.

In this study, the annual rate of events, λ(m>Mw), are determined based on the updated catalogue and compared to the GSC's MR relations. These comparisons are shown in Figure 7 for the hazard-significant source zones. The GSC models defining best, lower and upper estimates of the MR relations are consistent with the seismicity rates observed in the updated catalogue. The alternative parameter values of MR relations for important source zones within ~200 km of the target site are listed in Table 1.

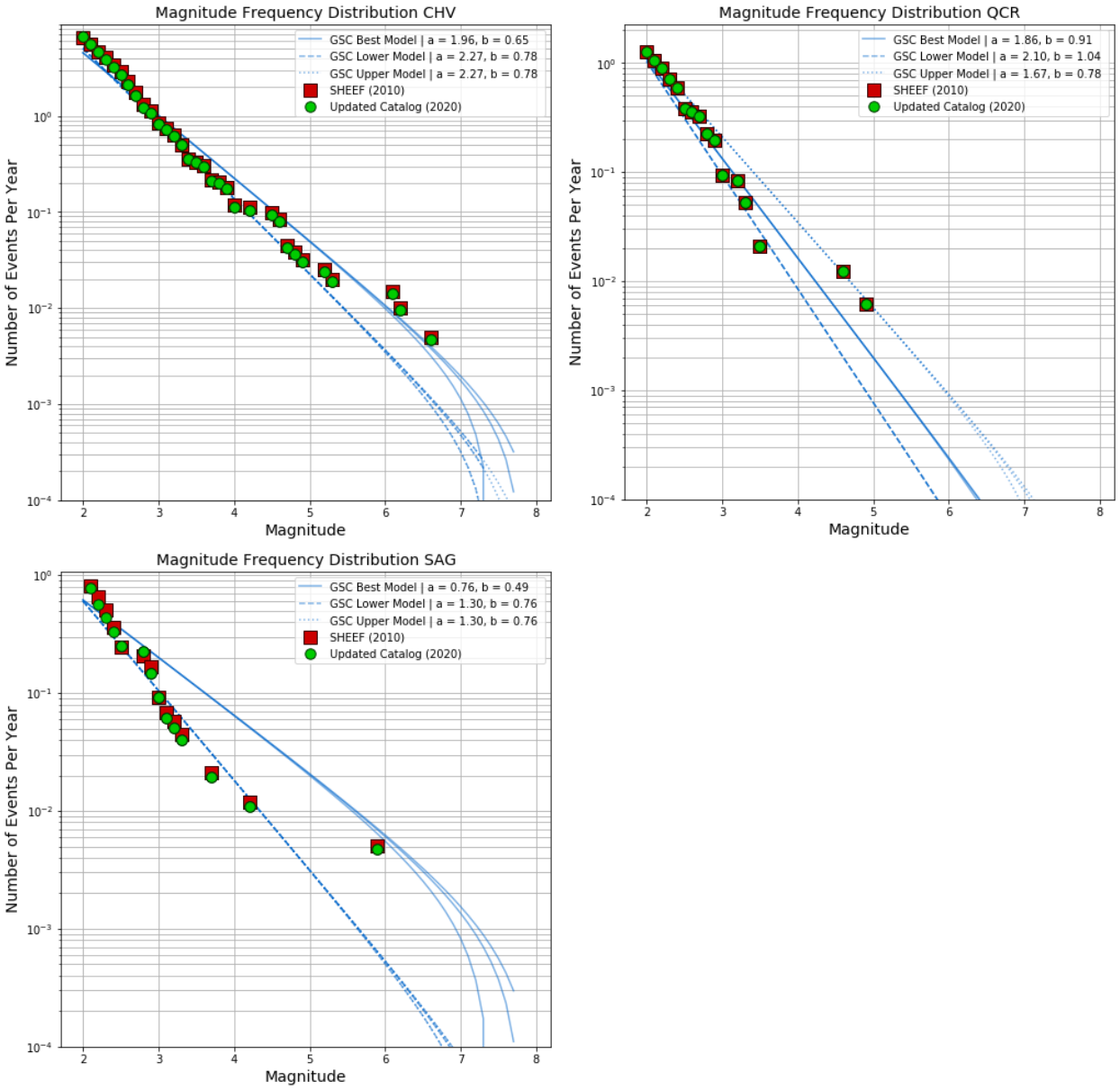

Figure 7. Comparison of GSC's MR relations (lines) and the annual rate of earthquakes (symbols), as determined from the updated regional catalogue, for hazard-significant source zones.

Table 1. Parameter values of GSC's MR relations for hazard-significant source zones

Source Zone	Model	a-value	b-value	Mx
CHV	Best:	1.96	0.65	7.8
	Lower:	2.27	0.78	7.4
	Upper:	2.27	0.78	8.0
SAG	Best:	0.76	0.49	7.8
	Lower:	1.30	0.76	7.4
	Upper:	1.30	0.76	8.0
QCR	Best:	1.86	0.91	7.8
	Lower:	2.32	1.14	7.4
	Upper:	1.45	0.69	8.0

The source models are used in hazard analysis in a logic-tree framework that is adopted from the 5th generation hazard model. It accounts for uncertainties in hypocenter depths, MR relations and maximum magnitudes using three alternative discretized branches with assigned weights (Figure 8). Consistent with the 5th generation hazard model, a minimum magnitude of Mw4.8 is used in the analysis.

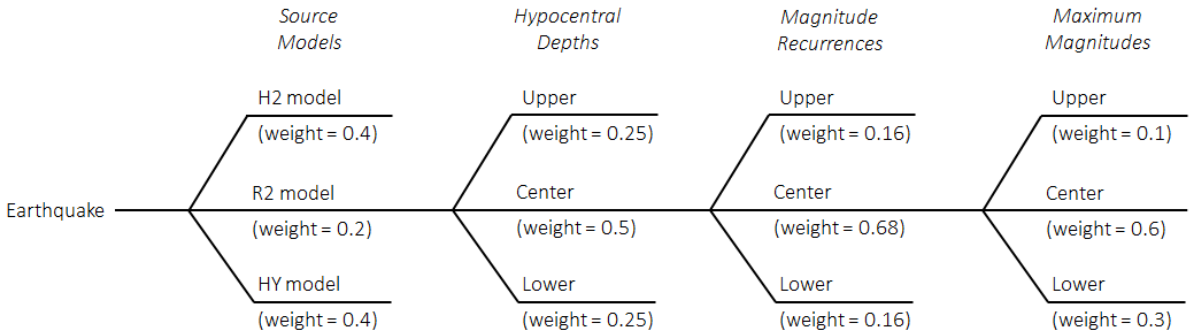

Figure 8. Illustration for the source model logic tree

5.4. Seismicity Potential in the Site Vicinity

Local Faults

Seismic sources in the adopted base model are defined as areal source zones. In general, it is difficult to associate observed seismicity with specific faults with confidence due to insufficient location accuracy and low activity rates, combined with the likelihood that earthquakes are happening on a diffuse series of unmapped faults at depth, rather than those seen on the surface. Earthquakes in eastern Canada typically occur at depths of 5 to 20 km, on faults that have no surface expression. Furthermore, faults mapped on the bedrock surface in Eastern Canada were formed hundreds of millions of years ago, and typically have no documented relation to current seismic activity. Thus, there is no clear-cut relationship between mapped bedrock faults and observed seismicity. The only known exception in Eastern Canada is the Ungava fault in northern Quebec, which was characterized by the occurrence of the 1989 M6.3

earthquake that produced surface rupture and subsequent aftershocks (Adams and Basham, 1991).

A fault map was acquired from the Quebec Geomine Information System (SIGEOM), hosted by Energy and Natural Resources Québec, which revealed the mapped extents of several large fault structures between Saguenay and Charlevoix (Figure 9). Most faults in the area are oriented in NW-SE or NE-SW directions. Faille des Ha! Ha! is one of the notable faults near the study site and extending ~100 km to the south.

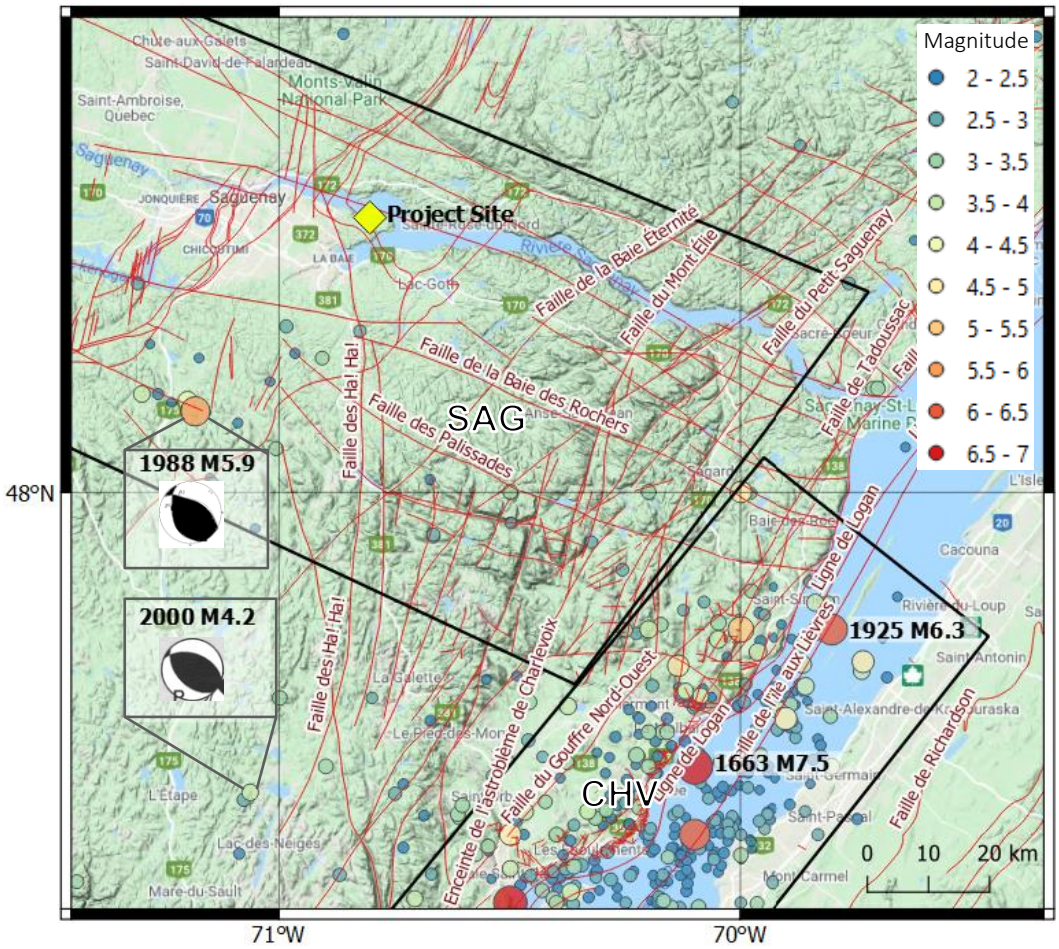

Figure 9. Surface extensions of known faults (red lines) in the vicinity of the site. All historical events of Mw>2 are shown. The 1988 Mw5.9 Saguenay, 1663 Mw~7.5 and 1925 Mw6.3 Charlevoix earthquakes are indicated on the map. Moment tensor solutions for the 1988 Mw5.9 event (Ma et al., (2018) and another earthquake of Mw4.2 (Bent, 2003) are also shown.

The SIGEOM database does not include information on the strike, dip, depth or mechanism of faults. However, focal mechanism solutions of recorded events can shed some light in terms of the predominant stress orientation and slip characteristics in the study area. Ma et al. (2018) performed high precision relocations on the 1988 Saguenay earthquake sequence and re-compute the rupture plane for the M5.9 event. The authors found a strike dip and rake of 299°, 57° and 64° respectively, indicating a reverse faulting mechanism which dips to the north east.

Another Mw4.2 earthquake located within the Jacques-Cartier block 60 km to the south of the 1988 M5.9 event, shares a similarly oriented reverse faulting mechanism with strike, dip and rake of 289°, 47° and 70° respectively (Bent and Perry, 2003). These orientations align with the predominantly north-east and south-west oriented maximum horizontal stress direction in the region determined from borehole measurements (Mazzotti and Townend, 2010).

Location of the 1663 M7.5 Earthquake

There is a debate on the true location of the 1663 M7.5 earthquake in the literature, which may have important implications in terms of seismic hazard in the study area. GSC locates this event in the Charlevoix seismic zone based on historical damage reports (Smith, 1962). However, Locat et al. (2003, 2009, 2011) proposed that the 1663 M7.5 earthquake was located near Saguenay based on observations of land and marine mass wasting events throughout the Saguenay Fjord. Locat et al. (2003) identified a surficial fault-like feature which intersects the Saguenay Fjord approximately 10km to the south west of the study site. The authors suggested that this feature might hosted the 1663 M7.5 earthquake. The feature displays a slip of 0.5m and a known length of 600m. A correspondence with Dr. Jacques Locat indicated that this feature may be a part of Faille de Ha! Ha! or a different unmapped fault in the area (Figure 10). Further field work would be required to determine the full extent of this feature and its relationship with known faults in the area.

In a more recent study, Turmel and Locat (2016) performed seismic wave propagation simulations for three proposed locations of the epicenter of the 1663 M7.5 event: (i) the location of the 1925 Charlevoix earthquake, (ii) the location of the 1988 Saguenay earthquake, and (iii) within the Baie des Ha! Ha!, roughly 10 km south west from the study site. Centroid moment tensor solutions from the 1925 and 1988 earthquake were scaled up to a M7.9 earthquake and the ground motion intensities that would be felt at the surface were simulated across the region. It was found that an epicenter at any of the three locations produced ground shaking intensities at the surface that were significant enough to have triggered the observed land and marine slides throughout the Saguenay Fjord. The moment magnitude events are scaled to in the study are on the high end of what Ebel (2011) estimated the moment magnitude of the 1663 event at M7.5 ± 0.5. Turmel and Locat (2016) do not consider site amplification effects of near surface sediment layers or local topography throughout the region. It is possible for these two reasons that that the ground motions generated in the simulations are not entirely representative of the 1663 event. The authors concluded that the location of the earthquake was more likely to be somewhere between the three proposed locations within the Jacques-Cartier Block rather than within the Fjord.

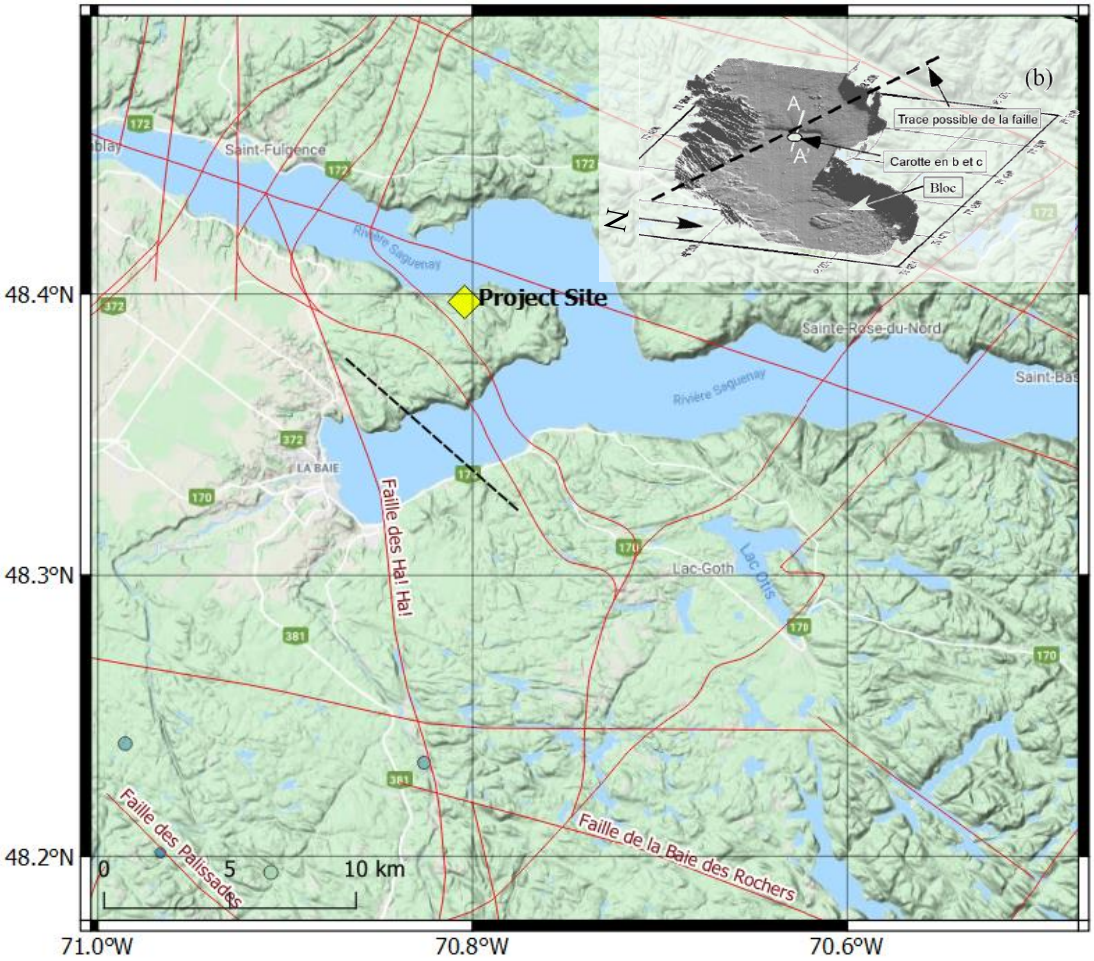

Figure 10. Locations of Faille de Ha! Ha! and the feature indicated by Locat et al. (2003) is shown (black dashed line and top-right inset), relative to the study site.

Return Period of Characteristic Earthquakes

An understanding of the return period of potential seismicity on the postulated faults in Saguenay region is required in order to assess whether they pose additional hazard at the study site. St Onge et al., (2004) studied rapidly deposited layers (RDL) in the Saguenay Fjord. They identified two RDLs that formed during the last 4000 years within the Fjord. The study indicated that the 1988 Mw5.9 Saguenay earthquake did not produce any significant land or marine slides within the Fjord. As a result, the authors suggest that an earthquake with Mw6.75 or greater would be required to form RDLs within the Fjord, if the event epicenter was located near the 1988 sequence. The return period of such event would be approximately 2000 years.

Tuttle and Cowie (1991) documented the characteristics of liquefaction features that formed during and before the 1988 Mw5.9 Saguenay earthquake. In the excavations of the 1988 sand boils in Ferland area (~20 km to the south of the study site), they found cross-cut liquefaction features from the pre-1988 period. These features were similar in morphology to the modern features and were therefore interpreted to be earthquake-induced liquefaction features. The

pre-1988 features in Ferland were larger than the equivalent features that formed during the 1988 earthquake. This suggests that the source of the earthquake responsible for their formation was located closer to Ferland and was probably different from the source that generated the 1988 Saguenay earthquake. The age of one pre-1988 feature was well-constrained an estimated age of 350 radiocarbon years. The youngest maximum age for another pre-1988 feature was dated to be approximately 1250 radiocarbon years. The authors pose two possible interpretations from these features. Either that two earthquakes large enough to induce liquefaction occurred in the Laurentide-Saguenay region during the 1250 radiocarbon years prior to the Saguenay event; or alternatively, that one such earthquake occurred in the region in the 400 radiocarbon years before 1988.

For the SAG seismic zone in the H2 source model, two recurrence parameter sets were developed by the GSC. The 'best' model (weighted 68%) was developed to capture the return period of the Mw5.9 event with a relatively low b-value of 0.49 to match the observed rate of M>2 earthquakes in the region. It corresponds to an upper boundary of return period in the range of 500-1000 years for a Mw7 earthquake, depending on the choice of maximum magnitude (Mx). The 'alternative' model (weighted 32%) captures the recurrence of the all other observed seismicity in the zone, returning a steeper b-value of 0.76. This model corresponds to a lower boundary of return period in the order of ~10,000 years for a Mw7 earthquake. Therefore, it is concluded that the GSC's recurrence models for SAG zone captures the ranges of return periods determined based on liquefaction events (Tuttle and Cowie, 1991) as well as the rapidly deposited layers found in Fjord (Tremblay et al., 2013).

Spatial Distribution of Potential Seismicity

While the uncertainty in return period of potential large events in SAG zone is captured by the GSC's recurrence models, their spatial distribution should also be accurately represented in order to ensure reliable hazard estimates. As shown in Figure 9, there are several faults in the study area, some of which are optimally oriented with the predominant stress regime and/or are in sufficient lengths to host moderate-to-large earthquakes. The literature review has indicated that one or more large earthquakes occurred in SAG zone before the 1988 sequence. However, the locations of these events are uncertain and it is not possible to associate those events to any particular fault(s) in the area. The paucity of recorded seismicity and their poor location accuracy poses additional challenge to sufficiently justify attributing any earthquakes onto each fault. No information found in the literature to suggest any of the faults to be more capable of generating seismicity than others.

The seismic source zone models developed by the GSC assume a uniform distribution of seismicity such that the probability of having an earthquake of any size is equivalent throughout the entirety of the zone. An alternative approach is to consider smoothed seismicity such that future seismicity is more likely to occur where seismicity has been observed in the past. Although observed seismicity in the Saguenay region is scarce, historical events overlay the mapped structures along the Saguenay rift margin and into the Jacques-Cartier Block between Saguenay

and Charlevoix (Figure 9). We apply smoothed seismicity to the H2 source model, and the associated zones within the HY source model in order to test the ability of the approach to constrain seismicity near faulted areas. We maintain the GSC's logic behind the R2 source model and associated zones within the HY source model such that seismicity could occur uniformly along any of the rift structures. We observe that the synthetic events generated based on smoothed seismicity method are well confined in the areas where mapped faults exist, which corresponds to areas where past seismicity has occurred. Conversely, gaps in synthetically generated seismicity are observed to the North/North East of the site within the rift structure where it has been suggested that the Saguenay graben structures are inactive (De Burger, 1991; Tremblay et al., 2013).

To validate that the spatial distribution of seismicity is accurately considered in the hazard analysis with smoothed seismicity approach, a sub-set of large structures within the area between Saguenay and Charlevoix are identified: Faille des Ha! Ha!, Faille de la Baie Éternité, Faille de la Baie des Rochers, Faille de la Baie Satine-Marguerite, and an unnamed north-west to south-east striking fault in the south east corner of the Saguenay zone (Figure 11). Synthetic events generated within 10km of the faults are collected, and their recurrence rates are computed. We find the recurrence of Mw≥7 earthquakes around each of the posed faults to be in the range of 1/4000 year to 1/10000 year. Considering that there may be other faults throughout the rift margin area that have not been mapped, we also define an area that encapsulates the known and potentially unmapped faults between Saguenay and Charlevoix area and find a return period of 1/1300 years for earthquakes with Mw≥7. These findings suggest that the application the smoothed seismicity method with the GSC's recurrence rates for the SAG source zone implicitly captures the hazard posed by potential seismicity that could occur on the known and unidentified structures near the site.

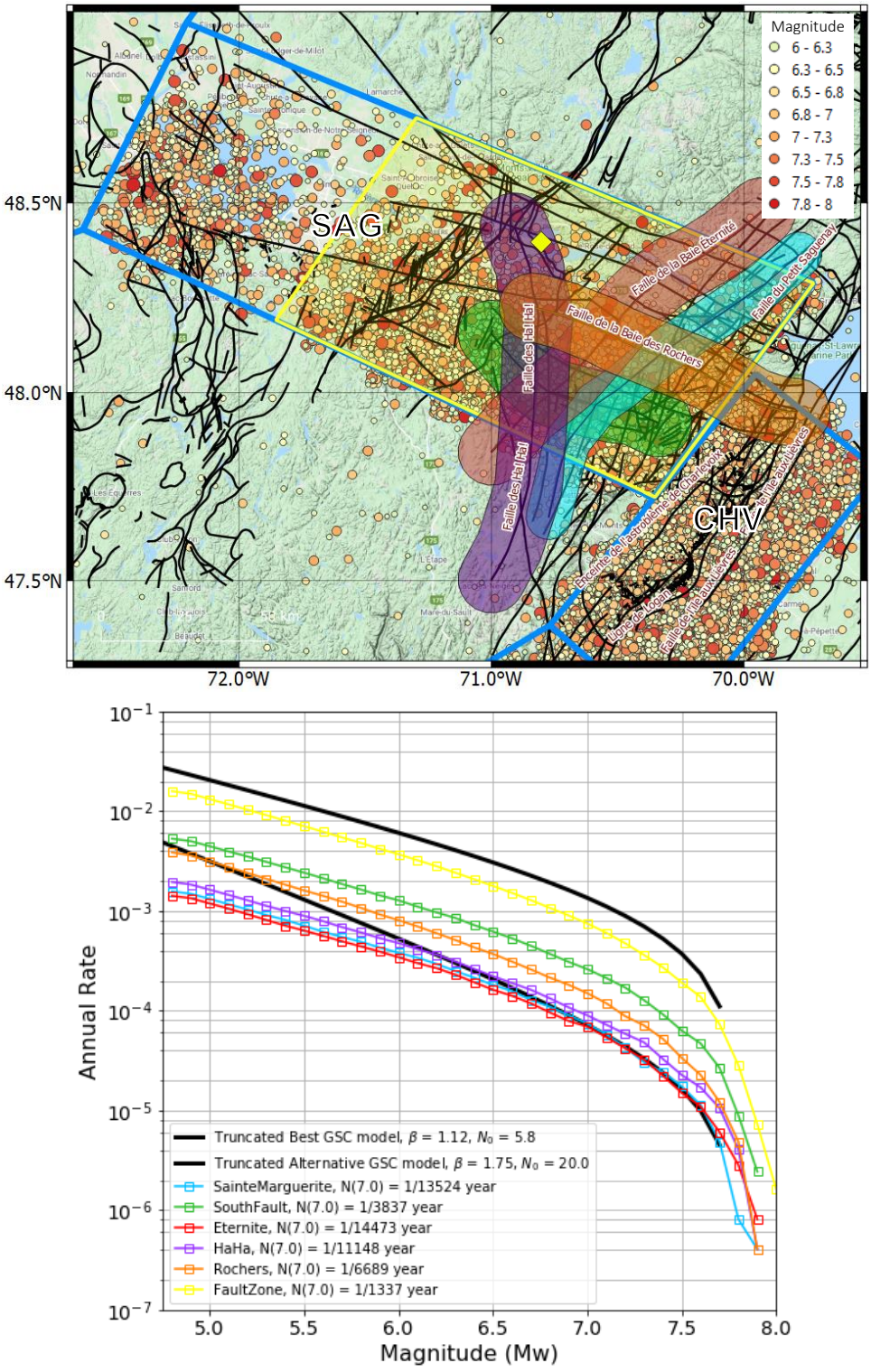

Figure 11. Map showing distribution of synthetic earthquake catalog generated based on smoothed seismicity method and pseudo-randomly selected fault orientations (upper). Recurrence parameters for individually selected faults and the broader fault zone (lower) suggest that the hazard posed by potential characteristic earthquakes across the zone is sufficiently captured by the implementation of smoothed seismicity method.

6. Ground Motion Model

6.1 GMM Approach

Two suites of GMMs are developed using the scaled-backbone approach (Atkinson et al., 2014). The essence of this approach is to identify one or more appropriate backbone GMMs that are consistent with the seismological attributes of earthquakes in the target region and to make adjustments as required, so that each model is transformed into a suite of alternative models that describe the center, body and range of median ground motions explicitly and transparently. This method is consistent with the original suggestions made in the Senior Seismic Hazard Analysis Committee (SSHAC) guidelines (Budnitz et al., 1997) and has been used widely in practice, including the 5th and 6th generation hazard models of Canada (Atkinson and Adams, 2013; Kolaj et al., 2019).

The first GMM suite is derived from the 17 seed models that were developed for hard-rock sites in Central and Eastern North America (CENA) in the NGA-East project (Goulet et al., 2018). The backbone model is determined as the weighted average of all NGA-East seed models. It is found to be in good agreement with the average ground motions recorded near the target site (Section 6.4). The epistemic uncertainty in median predictions is modeled based on a logic-tree approach, where the distribution of potential median predictions is approximated using a lower, central and upper model. The central model is represented by the backbone model and is scaled to define the lower and upper branch models. The scaling factor is determined based on the model-to-model differences considering all seed models, in which the priority is given to the hazard-significant magnitude and distance ranges (Section 6.5).

The second GMM suite is constructed based on the ground motion model of Atkinson et al. (2015, referred as Aea15 hereafter), which was derived for earthquakes in southern Ontario and western Quebec by a regional calibration of the CENA GMM of Yenier and Atkinson (2015) using recorded motions in the region. The Aea15 model provides ground motion estimates for hard-rock sites and is also found to be in good agreement with the average motions recorded in the site vicinity (Section 6.4). The epistemic uncertainty is modeled using logic tree branches about the Aea15 model based on the authors' recommendation of scaling factor (0.2 log units). The derived NGA-East and Aea15 GMM suites are presented in Section 6.6 and are given equal weights in the hazard analysis.

Aleatory variability of ground motions is treated independently from the specification of the median ground motions and associated epistemic uncertainty. The available data are insufficient to model aleatory variability with confidence. Consistent with the 5^{th} and 6^{th} generation hazard models, the representative aleatory variability values as proposed by Atkinson and Adams (2013) are used in this study. Adopted aleatory variability is 0.27 log units at long periods ($T \geq 1$ s), and decreases to 0.23 log units at short periods ($T \leq 0.25$ s).

6.2. Ground Motion Data

Earthquake ground motions are compiled from available monitoring stations in the vicinity of the project site. There are three public stations within the Saguenay area (CHIQ, LDAQ and SANQ) located 20 km, 60 km, and 90 km from the site respectively. Additionally, there are 13 stations located 100-150 km away in the Charlevoix area to the SE (Figure 12). The site conditions for the stations, where available, are described in Section 6.3. Earthquake ground motion records are compiled from IRIS continuous waveform data archives as well as from NRCan. Usable events of M>1 within 400 km of a station and occurred during the operational period of each station are identified and queried. The signal to noise ratio of the records are calculated during processing and used as a high-level filter to eliminate poor quality records.

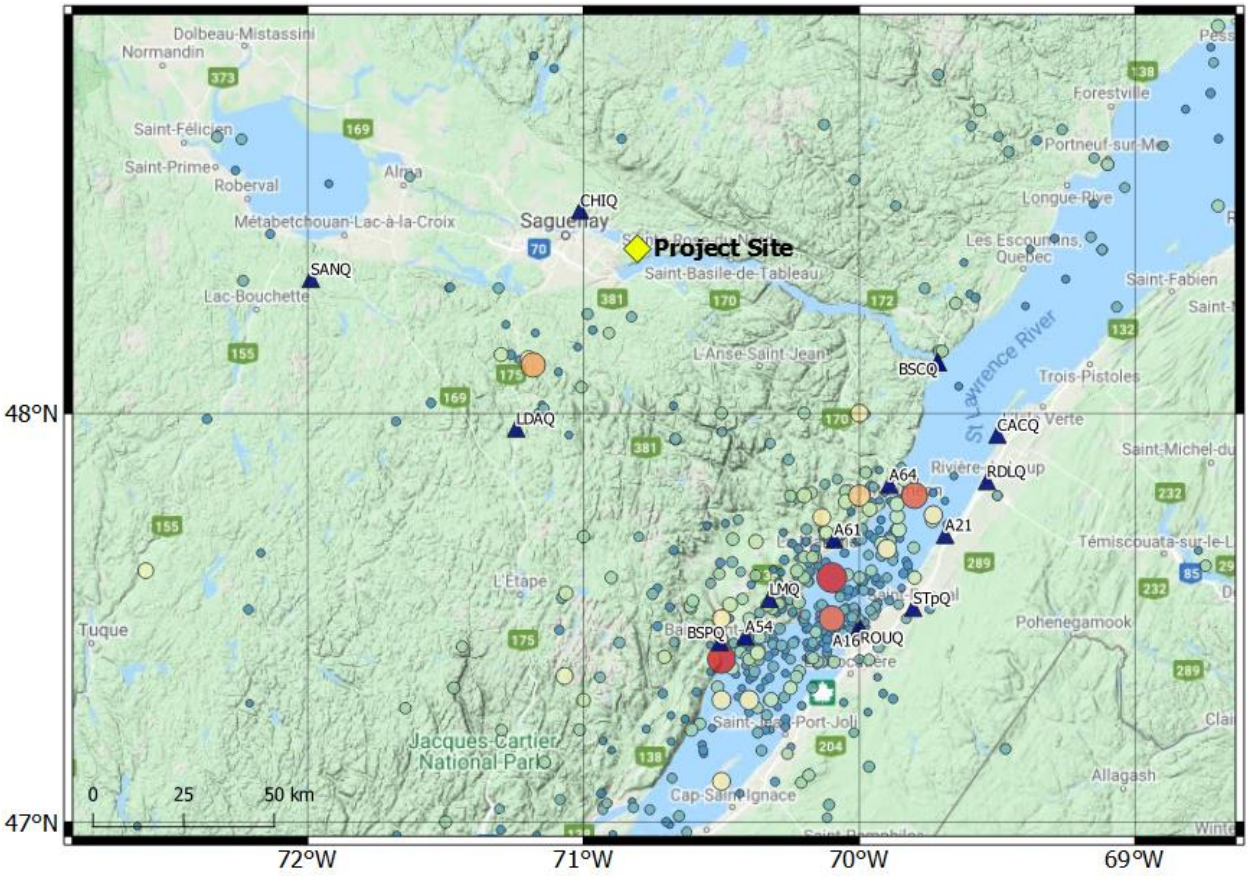

Figure 12. Seismic monitoring stations (triangles) operating near the target site. Earthquake catalog (circles) compiled in this study is also shown.

Compiled raw waveforms are processed in order to compute ground motion parameters. The processing routine includes windowing, trend removal, tapering, bandpass filtering and instrument response correction. For each record, the ground motion window of interest is identified based on estimated P and S arrival times. To this end, a regional travel-time model is developed. Manually picked P and S phase arrivals of past earthquakes are queried from the USGS database for all available event-station pairs in the region. Figure 13 shows ray paths of

event-station pairs used for the derivation of regional travel-time model. The regional travel-time relationships for P and S waves are shown in Figure 14 and provided in Equations 1 and 2, respectively:

$$t_p = \begin{cases} 0.15R_{hyp} + 1.01 & \text{for } R_{hyp} \leq 200 \text{ km} \\ 0.12R_{hyp} + 6.95 & \text{for } R_{hyp} > 200 \text{ km} \end{cases} \quad (1)$$

$$t_s = \begin{cases} 0.27R_{hyp} + 1.32 & \text{for } R_{hyp} \leq 200 \text{ km} \\ 0.23R_{hyp} + 9.29 & \text{for } R_{hyp} > 200 \text{ km} \end{cases} \quad (2)$$

where t_p and t_s are P- and S-wave travel times (s) and R_{hyp} is the hypocentral distance (km).

For a given earthquake record, the ground-motion window is defined from t_p to $t_p+4\Delta t_{sp}$ relative to the origin time, where Δt_{sp} is the S-P travel time difference. A 5-second buffer is considered at both ends of the ground-motion window to account for prediction uncertainties. This buffer is meant to ensure that the strong portion of ground motion is entirely captured. The length of the signal window used ranged from 20 sec to 200 sec, depending on the hypocentral distance. A pre-event noise window up to 30 s, where available, prior to the start time of the ground-motion window is included in the time series to quantify the quality of records. Figure 15 shows an example windowing of the ground-motion time series.

A linear trend line is subtracted from the raw waveform trace and a cosine taper is applied at each end. The resultant waveforms are then processed using a zero-phase shift 4th-order Butterworth bandpass filter. The low-pass frequency (f_{lp}) is defined as 80% of the Nyquist frequency in order to filter potential high-frequency noise as part of initial batch processing. The high-pass frequency (f_{hp}) is defined as $\log(f_{hp}) = 0.2 - 0.3Mw + 0.3\log(R_{hyp})$. This accounts for the dependence of signal-to-noise ratio on magnitude and distance. f_{hp} typically ranges from 0.4 Hz to 2.7 Hz for the processed waveforms. The instrument response is deconvolved from the recording by complex division in the frequency domain to ensure the accurate recovery of ground-motion amplitudes over a wide-frequency band.

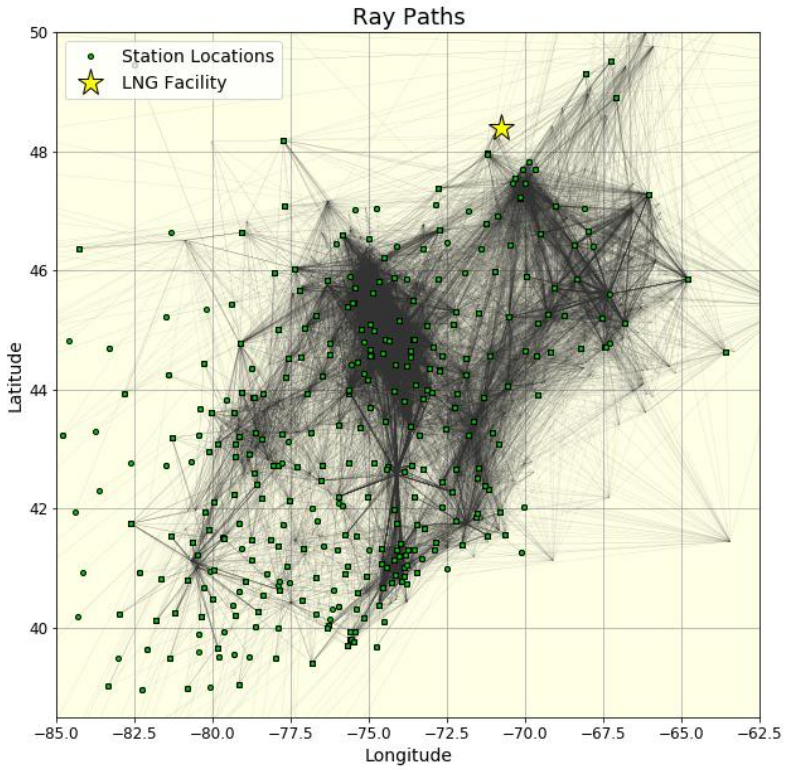

Figure 13. Ray paths of event-station pairs used for the derivation or regional travel-time model. Star represents the location of target site.

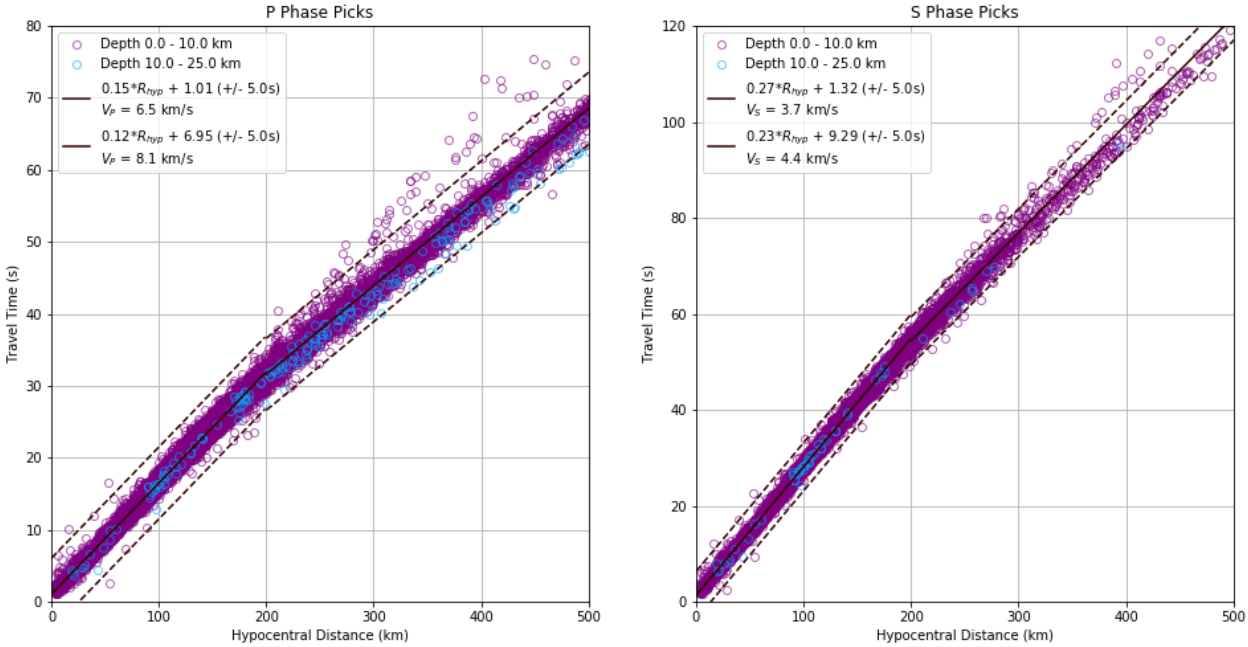

Figure 14. Travel-time models (solid lines) for P and S waves. Dashed lines indicate ±5 s around the estimated arrival times. Circles represent manual phase picks compiled from past events in the region.

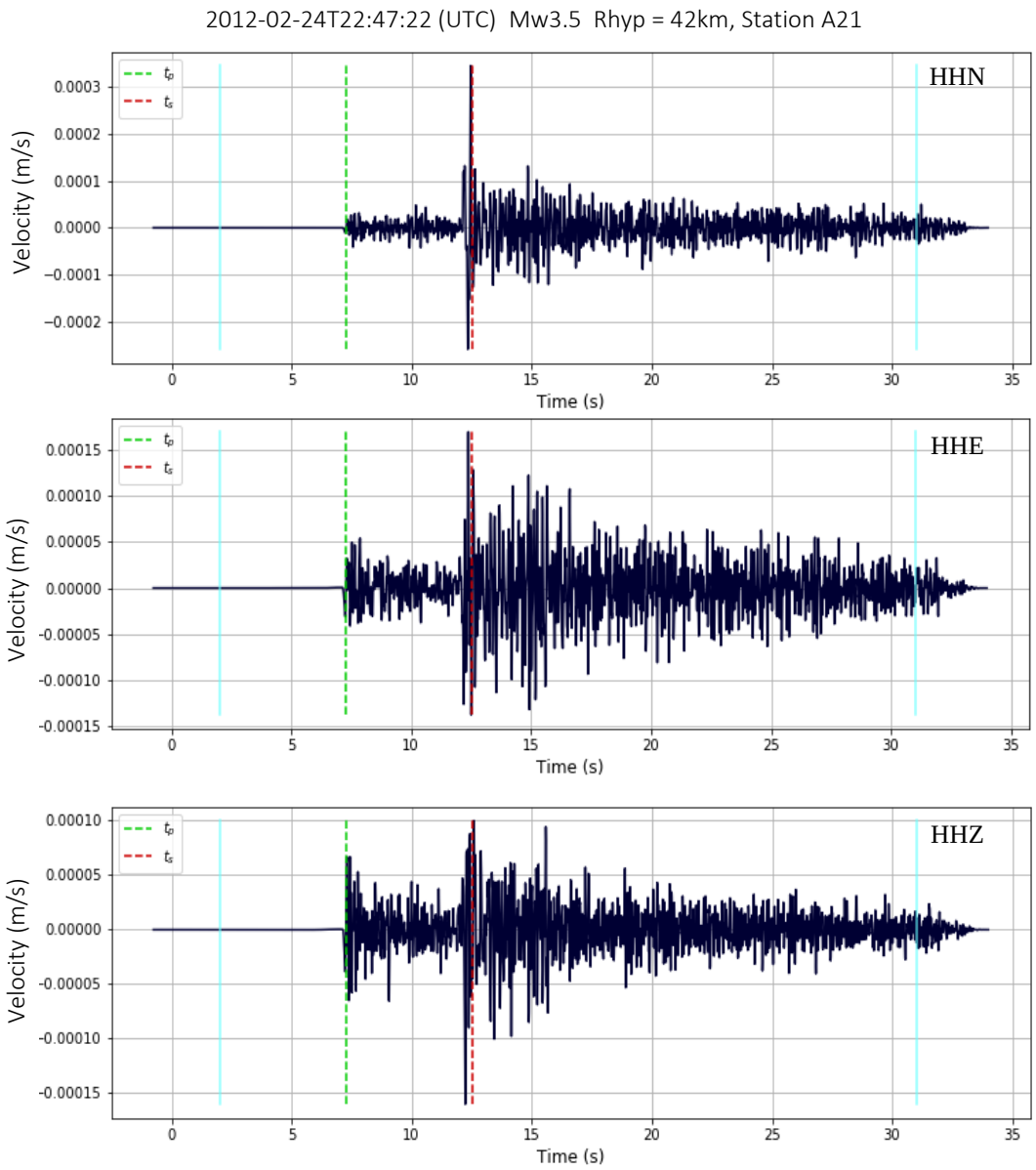

Figure 15. Example for the windowing of ground motion records. Estimated P and S arrivals are shown by green and red lines, respectively. Blue lines indicate the start and end times of ground motion window, including 5 s buffer at each end.

Finally, waveforms are visually inspected for record quality. Each record is assessed to determine if

a. windowing parameters need refinement,
b. the record has gaps or is incomplete within the ground-motion window of interest,
c. the record is too noisy and seismic arrivals cannot be distinguished, or
d. the waveforms are clipped due to the limited dynamic range of recording instrument.

Peak ground acceleration (PGA), peak ground velocity (PGV) and 5%-damped pseudo spectral acceleration (PSA) for periods up to the maximum usable period (0.8/fhp), are computed for each usable component. Figure 16 shows the distribution of usable ground motions (signal-to-noise ratio, SNR > 3). The majority of records are obtained from 1.0 < Mw < 3.0 events in the Charlevoix zone; there are a limited number of records from larger magnitudes, including the 1988 Mw5.9 Saguenay earthquake.

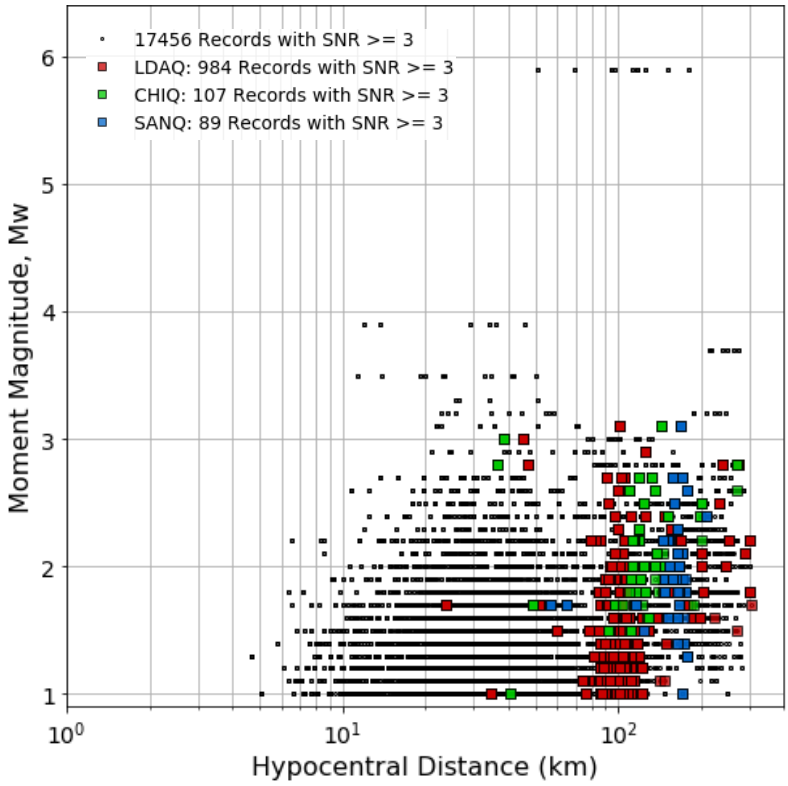

Figure 16. Magnitude-distance distribution of usable ground motions where the number in the legend indicates the number of individual channels with a signal to noise ratio greater than 3.

6.3. Site Condition

Site characteristics of the seismic stations within the Saguenay and Charlevoix regions are investigated in order to understand the compatibility of their ground motion recordings with the target site condition (Class A, hard rock). Based on the near surface shear-wave velocities reported by Palmer and Atkinson (2020) as well as the station site descriptions provided by Munro and North (1989), it is concluded that the majority of stations used in this study are located on hard rock site conditions, except the BSPQ station, which is found to be located on an alluvial fill.

The backbone GMMs adopted in this study were developed for hard-rock sites ($V_{S30} \geq 2000$ m/s). In practice, GMMs are typically adjusted to the target site condition in order to account for the

systematic differences in site amplification and high-frequency spectral decay. Recently, Palmer and Atkinson (2020) found that rock-to-hard rock sites (1200 m/s < V_{S30} < 3000 m/s) in southern Ontario and western Quebec have similar ground-motion attributes regardless of variations in their velocities. In order to further investigate whether the backbone GMMs are compatible with the target site condition, ground motions compiled in the site vicinity at known hard rock stations are compared with the predictions of backbone GMMs (discussed in the next section).

6.4. Comparison of Recorded Motions with GMMs

One of the major advancements in modeling of ground motions in ENA is the NGA-East project, which resulted in 17 mutually exclusive and completely exhaustive seed models for prediction of ground motions in CENA. The seed models were developed for hard rock sites (V_{S30} = 3000 m/s) and were provided in tabular format for magnitudes between 4.0 ≤ Mw ≤ 8.2 and distances up to 1500 km for peak ground acceleration (PGA), peak ground velocity (PGV) and 5% damped pseudo spectral accelerations (PSA) at 23 logarithmically spaced oscillator periods (0.01 s ≤ T ≤ 10 s). For Eastern Canada, GSC used the NGA-East seed models in the 6th generation hazard model, in addition to the Atkinson and Adams (2013) model as adopted from the 5th generation hazard model (Kolaj et al., 2019).

In this study, the weighted mean of 17 NGA-East seed models is adopted as a backbone model for the derivation of a GMM suite. It is determined based on the weights for individual seed models as recommended by Goulet et al. (2018). Additionally, the Atkinson et al. (2015, referred as Aea15) model, which was developed for 3.0 ≤ Mw ≤ 8.0 events recorded on hard rock sites (V_{S30} ≈ 2000 m/s) in southern Ontario and western Quebec, is also used as an alternative backbone model for the generation of a second GMM suite, that is directly applicable to the site region.

The two backbone models are compared against the compiled ground motion dataset in order to assess the regional compatibility of the adopted models. The NGA-East backbone model is extrapolated for 3.0 ≤ Mw < 4.0 events (assuming the same magnitude scaling from Mw 3 to 4 as that from Mw 4 to 5) in order to maximize the use of available ground motion data. Figures 17 and 18 show ground motion residuals (i.e., log(observed/predicted)) determined based on the two backbone models. Both backbone models attain near zero average residuals across all periods. Overall, the NGA East backbone model shows slightly better agreement with the observed motions in comparison to the Aea15 model. The agreement of the regional ground motion observations with the GMMs for hard rock is consistent with the findings of Palmer and Atkinson (2020) that rock sites in Eastern Canada have similar responses regardless of variations in their velocities. We conclude that both backbone GMMs are compatible with the target reference site and no site-specific adjustments are required.

It is noteworthy that the ground motions of 1988 Mw5.9 Saguenay earthquake (red circles in Figures 17 and 18) systematically attain large residuals in comparison to the both backbone

GMMs. This discrepancy is mainly attributed to the high stress drop of the 1988 event relative to the average stress drop of earthquakes in Central and Eastern North America (Boore and Atkinson, 1992). A further investigation is conducted to ensure that the uncertainty considered in GMM suites is wide enough to accommodate ground motions of this event.

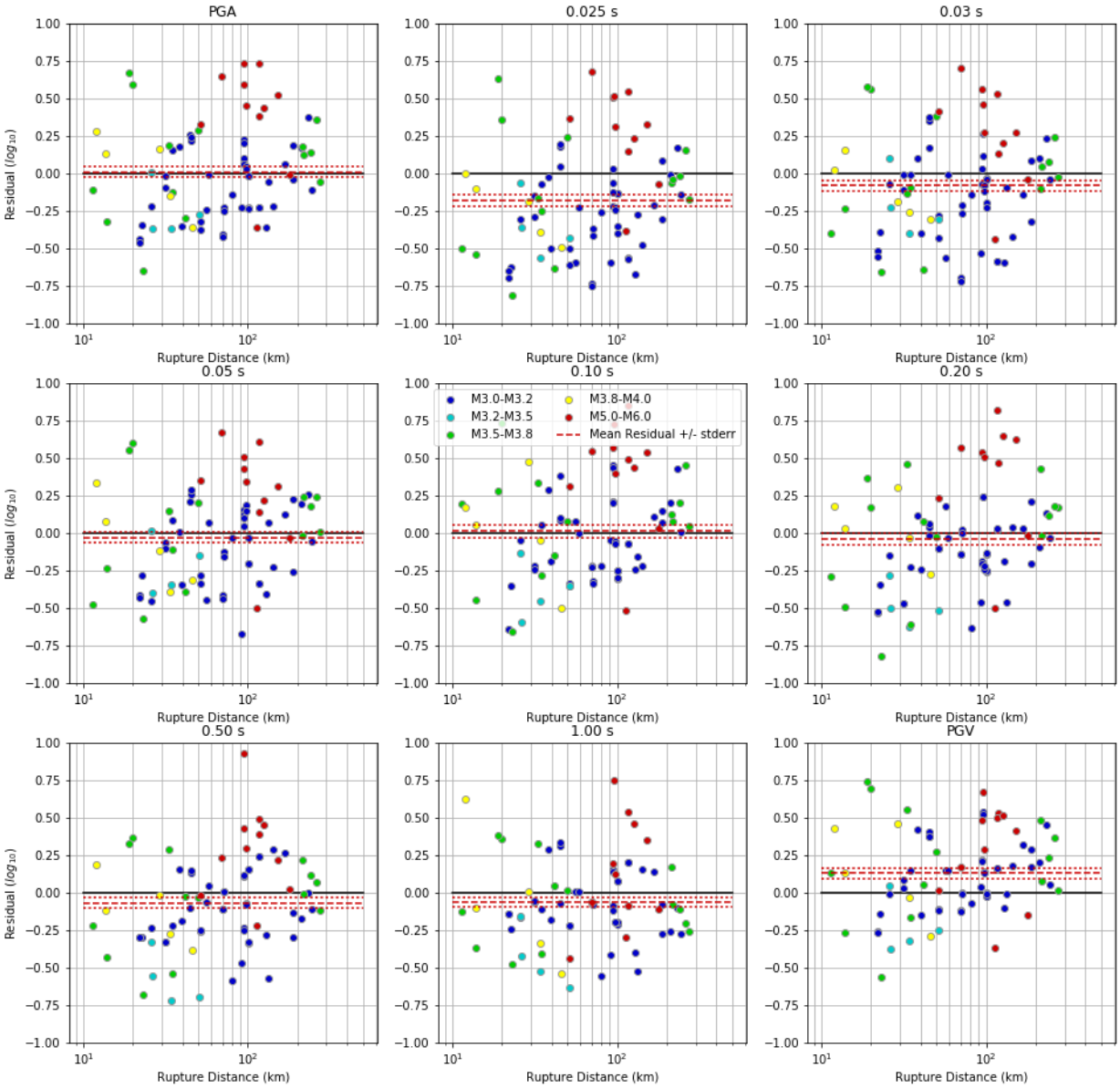

Figure 17. Ground motion residuals for NGA-East backbone (weighted mean) model. Dashed lines represent mean residuals and dotted lines indicate one standard error around the mean.

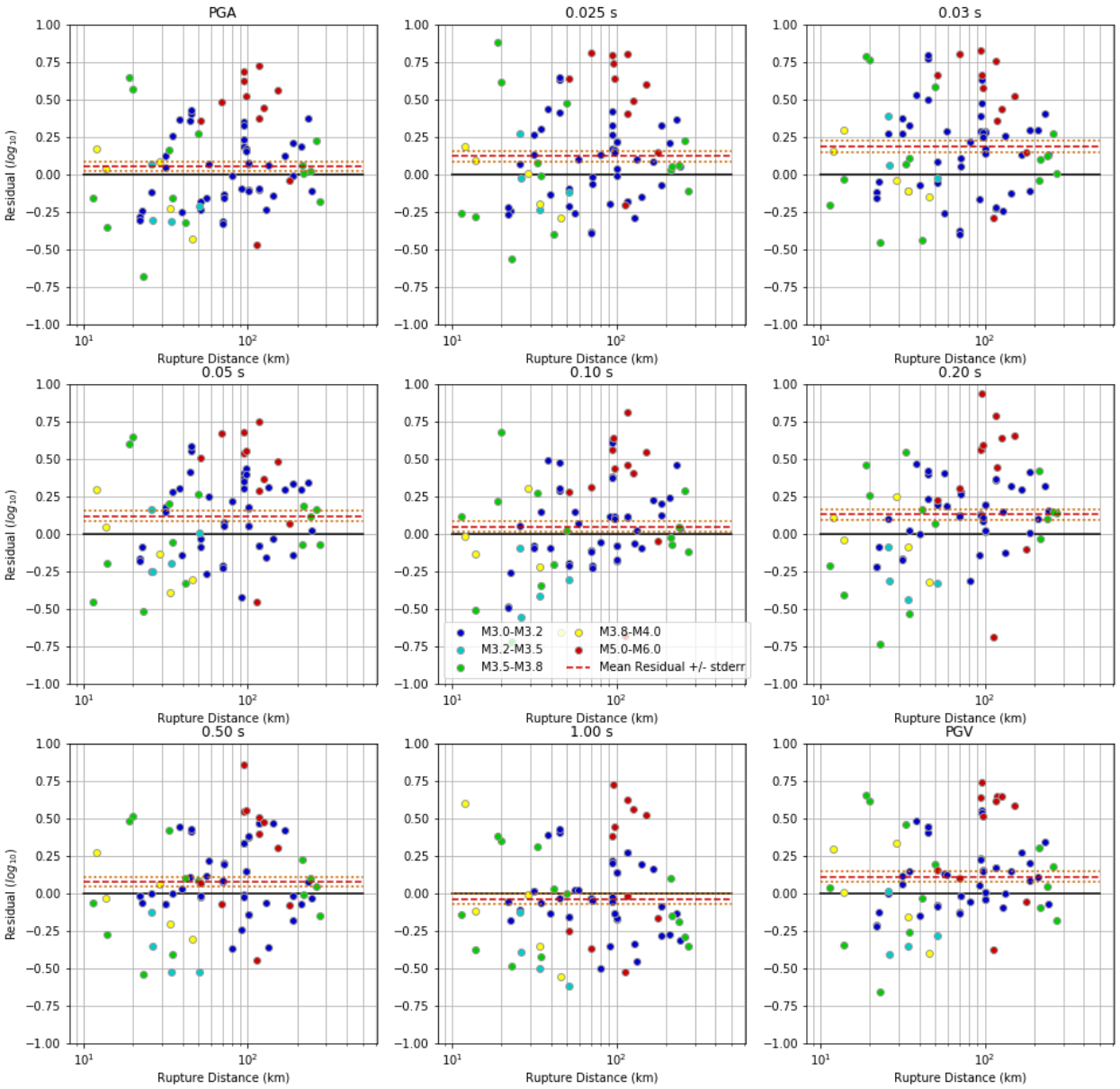

Figure 18. Ground motion residuals for Atkinson et al. (2015) backbone model. Dashed lines represent mean residuals and dotted lines indicate one standard error around the mean.

6.5. Epistemic Uncertainty

The epistemic uncertainty in median predictions of the NGA-East backbone model is quantified based on the model-to-model differences, considering the full set of seed models. Hazard-significant earthquake scenarios are considered in this assessment. Figure 19 shows disaggregation of 5th generation hazard estimates at the site for a return period of 2475 years, as obtained from GSC. It indicates that events within 100 km of the site, regardless of their magnitude, contribute most to the hazard. The hazard contribution of further events increases with spectral period.

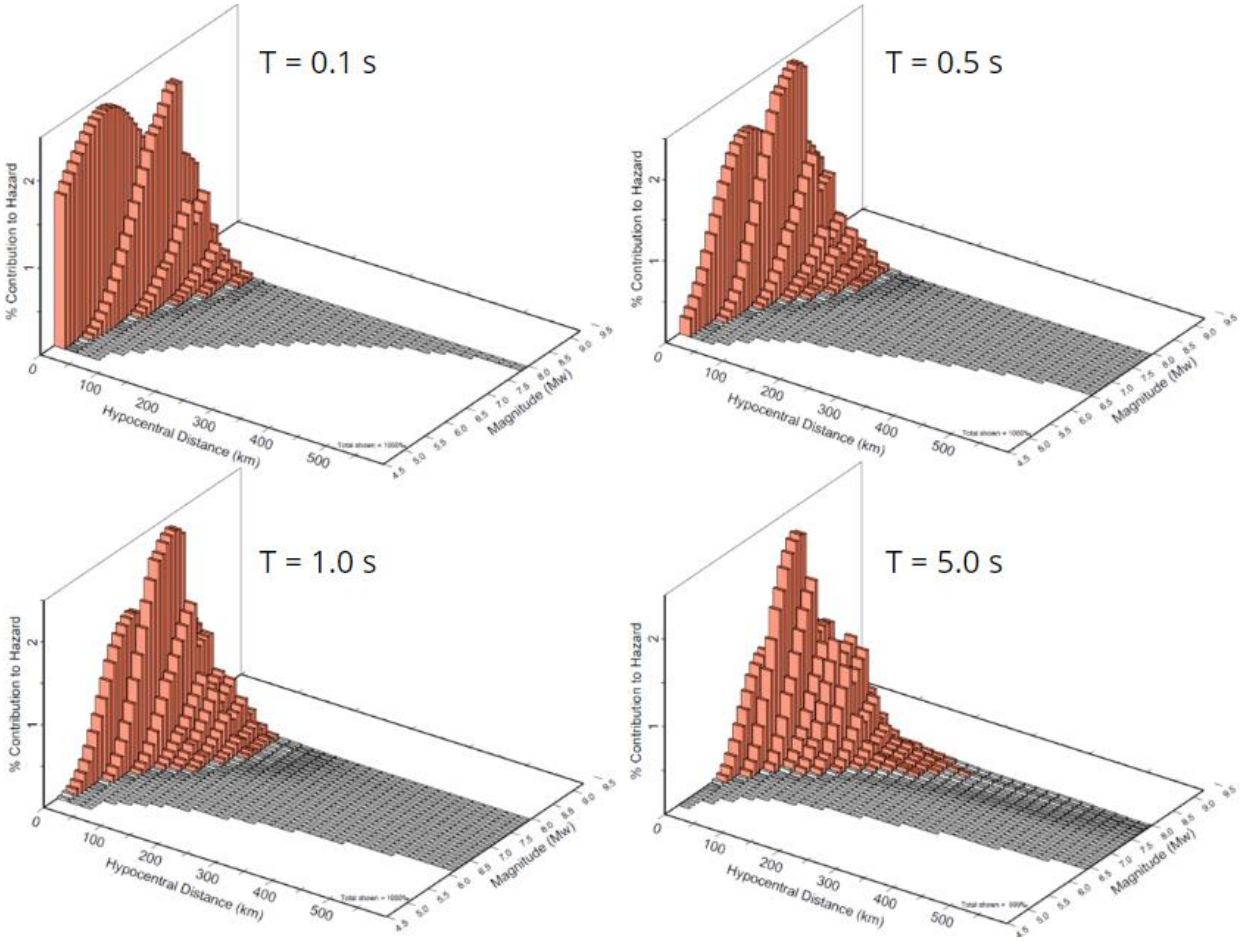

Figure 19. Hazard contributions from alternative magnitudes and distances for 2475-year return period, based on the 5th generation hazard model of GSC.

The variance of the NGA-East seed models is determined as a function of magnitude and distance. As shown in Figure 20, the variance is lower where empirical data are the richest in the NGA-East database and increases with magnitude and distance. Complexities in the model variability across different periods require some smoothing in order to avoid abrupt changes in the spectral shape of resultant GMM suites. With this in mind, standard deviations of the NGA-East seed models are computed across all periods, for different magnitudes and four distance ranges (Figure 21). Considering the hazard-significant earthquake scenarios, an epistemic uncertainty model (ε) that broadly captures the standard deviations across 4.0 < Mw < 8.0 within 100 km is derived as:

$$\varepsilon = \begin{cases} 0.128 & \mathrm{M_w} < 5.5 \\ 0.052\mathrm{M_w} - 0.16 & 5.5 \leq \mathrm{M_w} < 7.8 \\ 0.250 & \mathrm{M_w} \geq 7.8 \end{cases} \quad (3)$$

Epistemic uncertainty for the Aea15 model is adopted as 0.2 log units for all magnitudes, distance and periods based on author's recommendation. It is consistent with the average uncertainty observed in the NGA-East seed models.

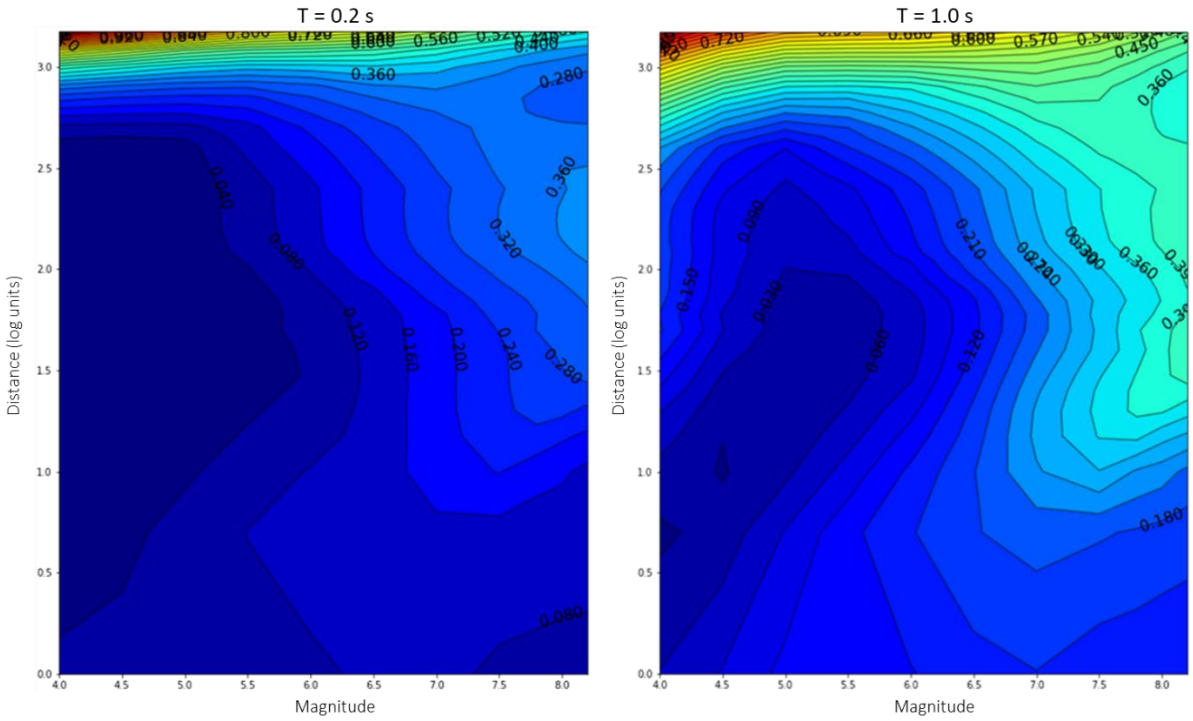

Figure 20. Variance of the NGA East seed models for spectral period T = 0.2 (left) and T = 1.0 s (right). Distances as well as contour lines are in log units.

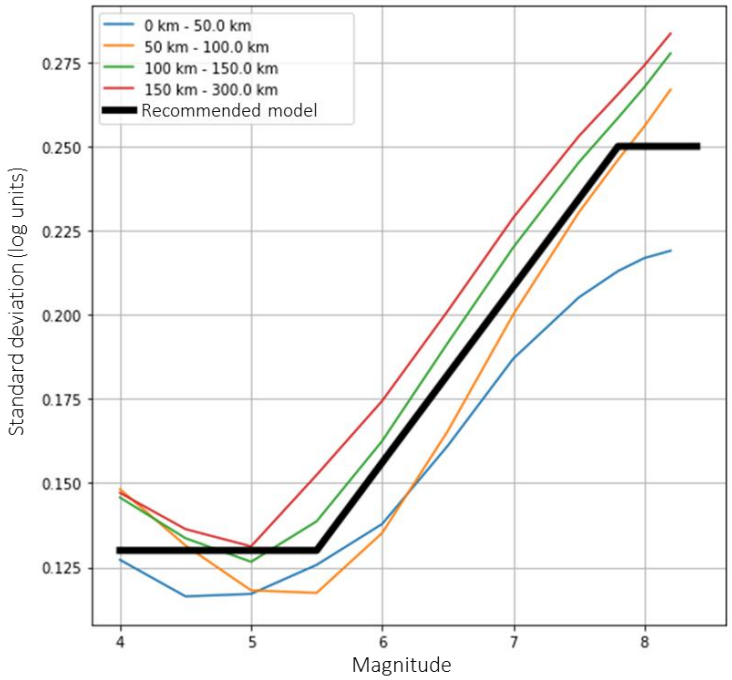

Figure 21. Standard deviation for NGA-East seed models, as determined across all periods for different magnitudes and four distance ranges. Standard deviation recommended for this study is also shown.

6.6. Ground Motion Model Suites

Two GMM suites that capture the epistemic uncertainty in median predictions are generated for use in hazard analysis. For each GMM suite, three alternative models (lower, central and upper) are defined using a logic-tree approach (Figure 22). The weighted-mean NGA-East and Aea15 models are used as central branches and each GMM is scaled up and down by 1.65ε to determine the corresponding upper and lower branches. This corresponds to a 90% confidence interval around each central model. Both GMM suites are given equal weights, with 0.6, 0.2 and 0.2 weights for central, upper and lower branches within each suite. Figure 23 shows a comparison of the GMM suites developed in this study.

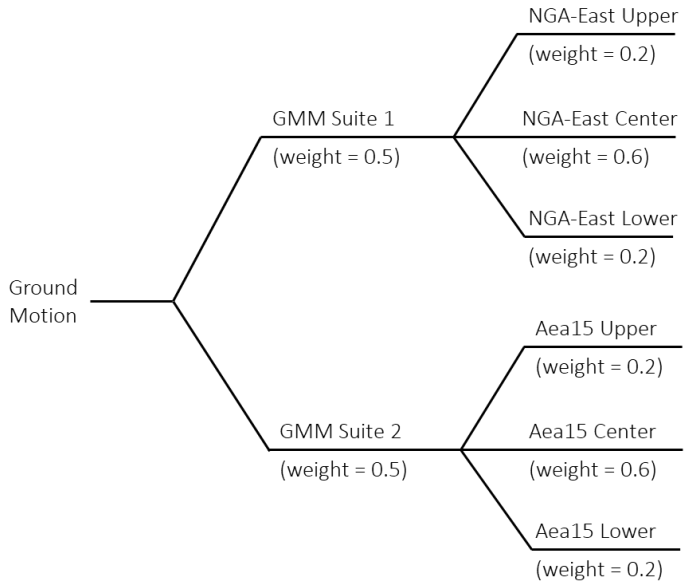

Figure 22. Ground motion logic tree

As discussed earlier, ground motions of the 1988 Mw5.9 Saguenay earthquake exhibit anomalously large values in comparison to the average motions observed from similar sized event in Central and Eastern North America. This is attributed to the high stress drop of the 1988 event. We examine whether the ground motion uncertainty modeled by different branches of GMM suites reasonably captures the large ground motions of the 1988 earthquake. This is shown in Figure 24, which indicates that no further modification is required for the GMM suites.

The derived GMM suites provide estimates of geometric-mean horizontal ground motions (PGA and PSA for periods from 0.01 to 10 s), for generic hard rock sites (Class A) in Eastern Canada and are shown compatible with average motions recorded in the site vicinity (Figures 17 and 18). They account for the epistemic uncertainty due to alternative interpretation and modeling of source, attenuation and site effects. Seismic hazard is computed independently for each spectral period and PGA using GMM suites derived in this study.

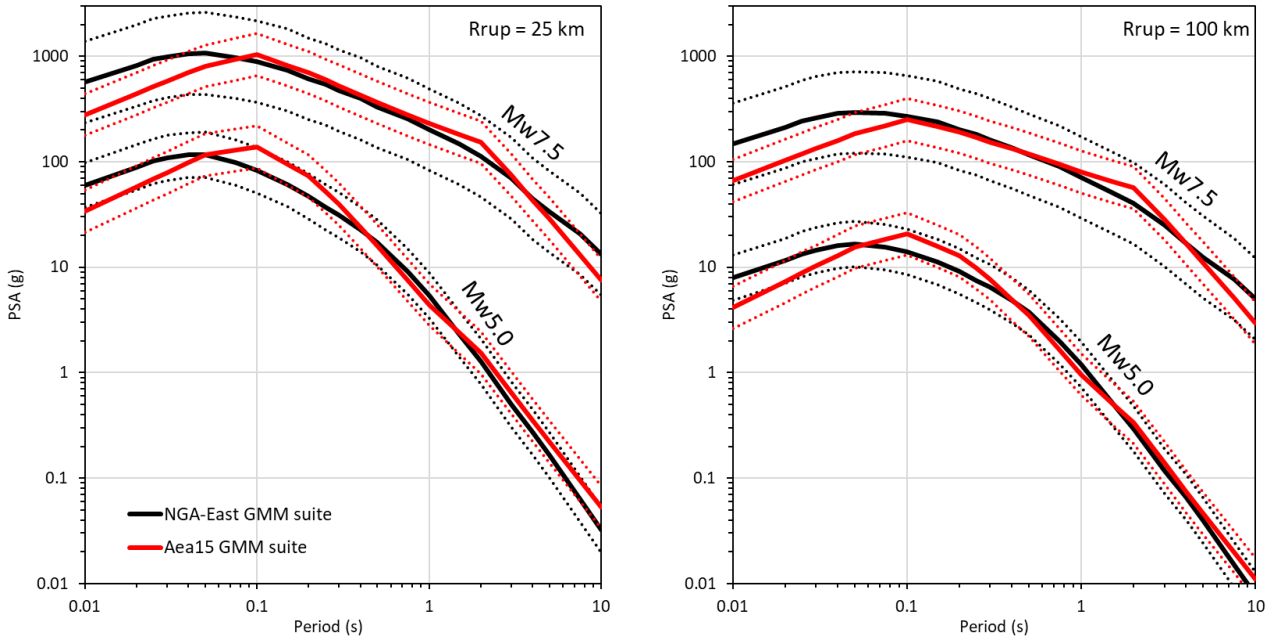

Figure 23. GMM suites used in the hazard analysis. PSA values are plotted for Mw5 and Mw7.5 events at 25 km and 100 km from the target site. Solid lines represent center models and dotted lines indicate lower and upper models.

6.7. Aleatory Variability

Aleatory variability represents the random scatter of ground motion observations. In the past, aleatory variability was assigned based on observed variability about the ground motion models using the available data. However, it has been realized this may not be the most appropriate way to define aleatory variability. Factors such as model misfits, variable soil conditions, data errors contribute to reported values for regression statistics, but are not representative of actual physical variability. When epistemic uncertainty in the median equations is included in hazard analysis there is also potential for some double counting of aleatory uncertainties. Papers by Anderson and Brune (1999), Anderson et al. (2000); Abrahamson and Bommer (2005), Atkinson (2006, 2011) and Strasser et al. (2009) discuss these issues in detail. In those studies, it is proposed that aleatory variability is best defined based on active crustal regions, where empirical data is abundant and is applicable to all event types and regions (Atkinson, 2013). With this in mind, the representative aleatory variability proposed by Atkinson and Adams (2013) is adopted in this study. It attains 0.27 log units at long periods ($T \geq 1$ s), and decreases to 0.23 log units at short periods ($T \leq 0.25$ s).

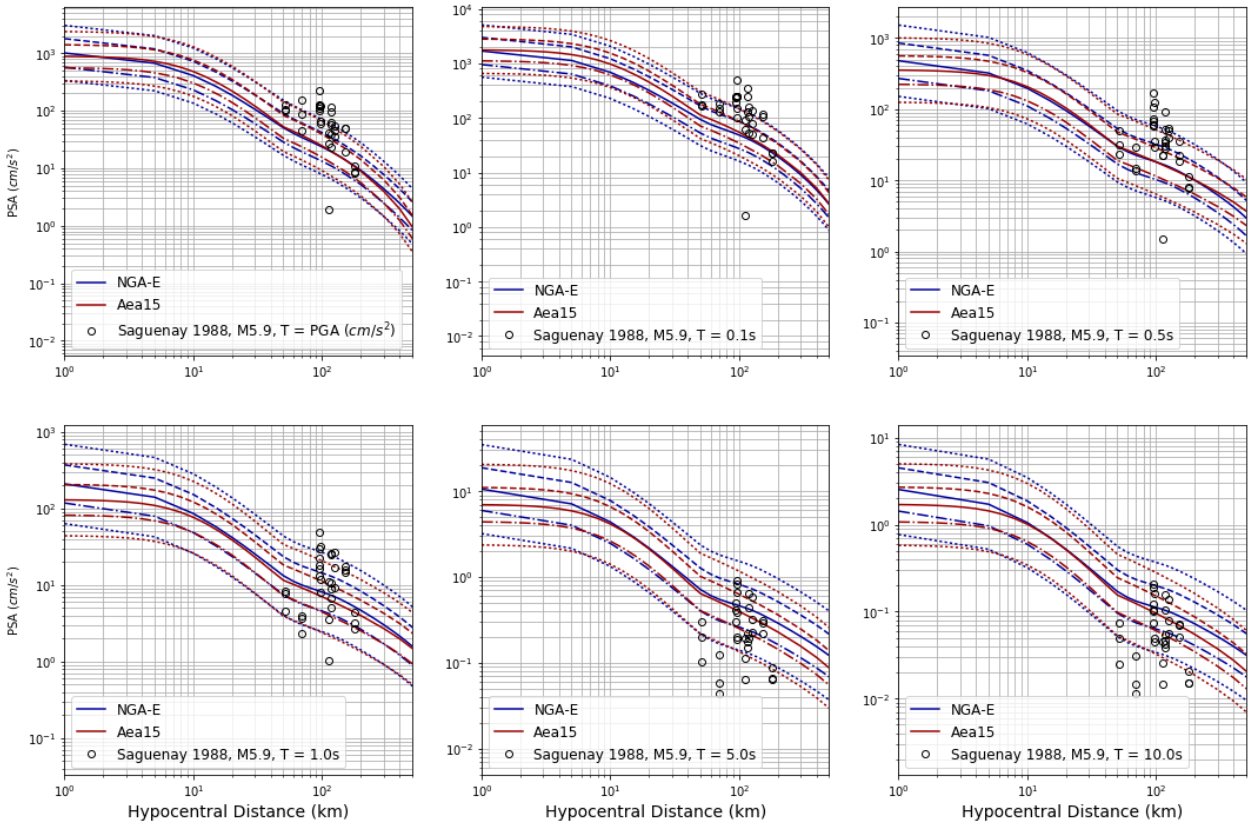

Figure 24. Comparison of the ground motions of the 1988 Mw5.9 Saguenay earthquake (circles) and the derived GMM suites (lines) for PGA (top left) and PSA at different periods (as labeled in the legend of each panel). Solid and dashed lines represent the center, upper and lower branches of each GMM suite (NGA-East and Aea15). Dotted lines indicate after upper and lower branches after the addition of aleatory variability.

7. Hazard Analysis

The EqHaz software package (Assatourians and Atkinson, 2013) is used for the calculation of ground motion hazard at the study site. First, a preliminary analysis is performed using the 5th generation hazard model of GSC (Halchuk et al., 2015) and EqHaz results are validated against the GSC's hazard estimates at the study site. Next, the site-specific hazard analysis is performed using the 5th generation source model (with smoothed seismicity method) and the derived GMM suites in this study. Figure 25 shows the mean hazard curves calculated for hard rock (Class A) ground motions at the target site.

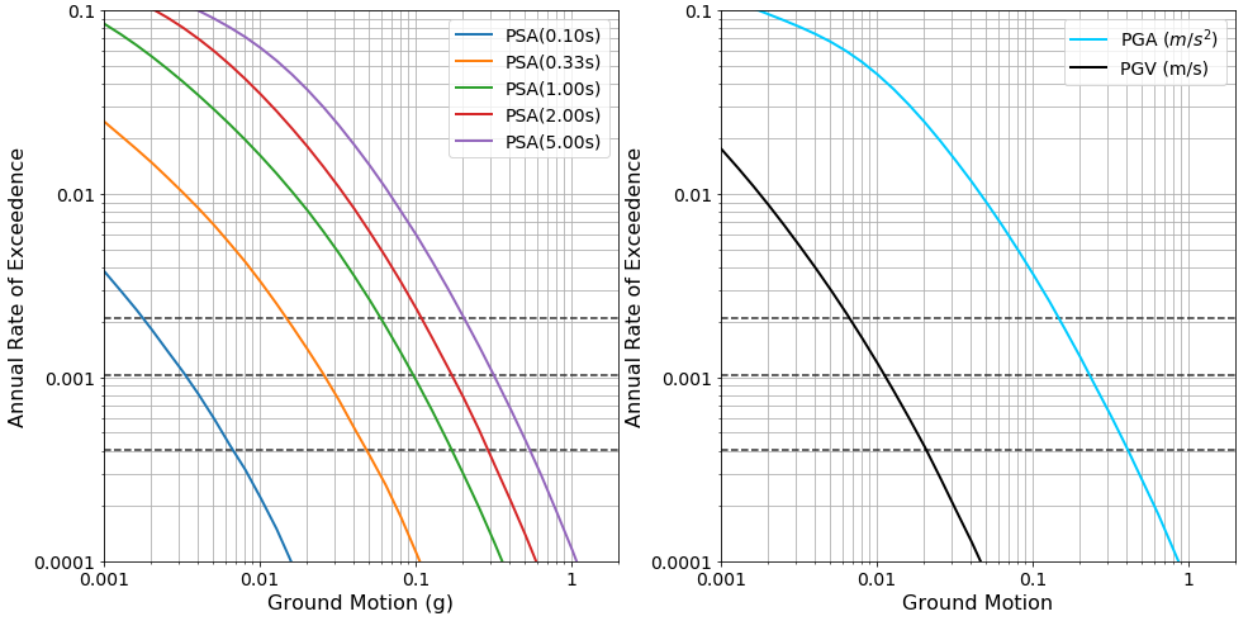

Figure 25. Hazard curves calculated hard rock (Class A) ground motions at the target site. Horizontal dashed lines show annual rate of exceedance at 1/475, 1/975 and 1/2475.

Figures 26 shows the horizontal-component uniform hazard spectra (UHS) determined for hard rock condition (Class A) at the target site for three return periods: 475, 975 and 2475 years. The site-specific UHS values are greater than the GSC's published values for the location based on the reginal 5th generation model, for all return periods. However, the UHS obtained in this study is generally equal or less than the GSC's preliminary UHS values based on the 6th generation model (Kolaj et al., 2020), for most periods (except 0.6 s < T < 4 s). This comparison could be done only for 2475-year return period because the 6th generation hazard estimates for other return periods have not been published at the time of this project. The observed differences between the results presented in this study and the 5th generation hazard model are attributed to a combination of the use of updated ground motion models as well as the implementation of smoothed seismicity method. The ground motion models (Atkinson et al., 2015 and NGA-East model suite) and epistemic uncertainties used in this study result in higher ground motion levels for the same magnitude-distance combination in comparison to the ground motion model used in the 5th generation hazard model (Atkinson and Adams, 2013). Additionally, the use of smoothed seismicity method resulted in concentration of potential seismicity around the areas

closer to the site where faults are concentrated and past seismicity has been observed, in comparison to the uniform distribution of potential seismicity considered by the GSC. These factors resulted in an increase in hazard estimates in comparison to the 5th generation hazard estimates of GSC.

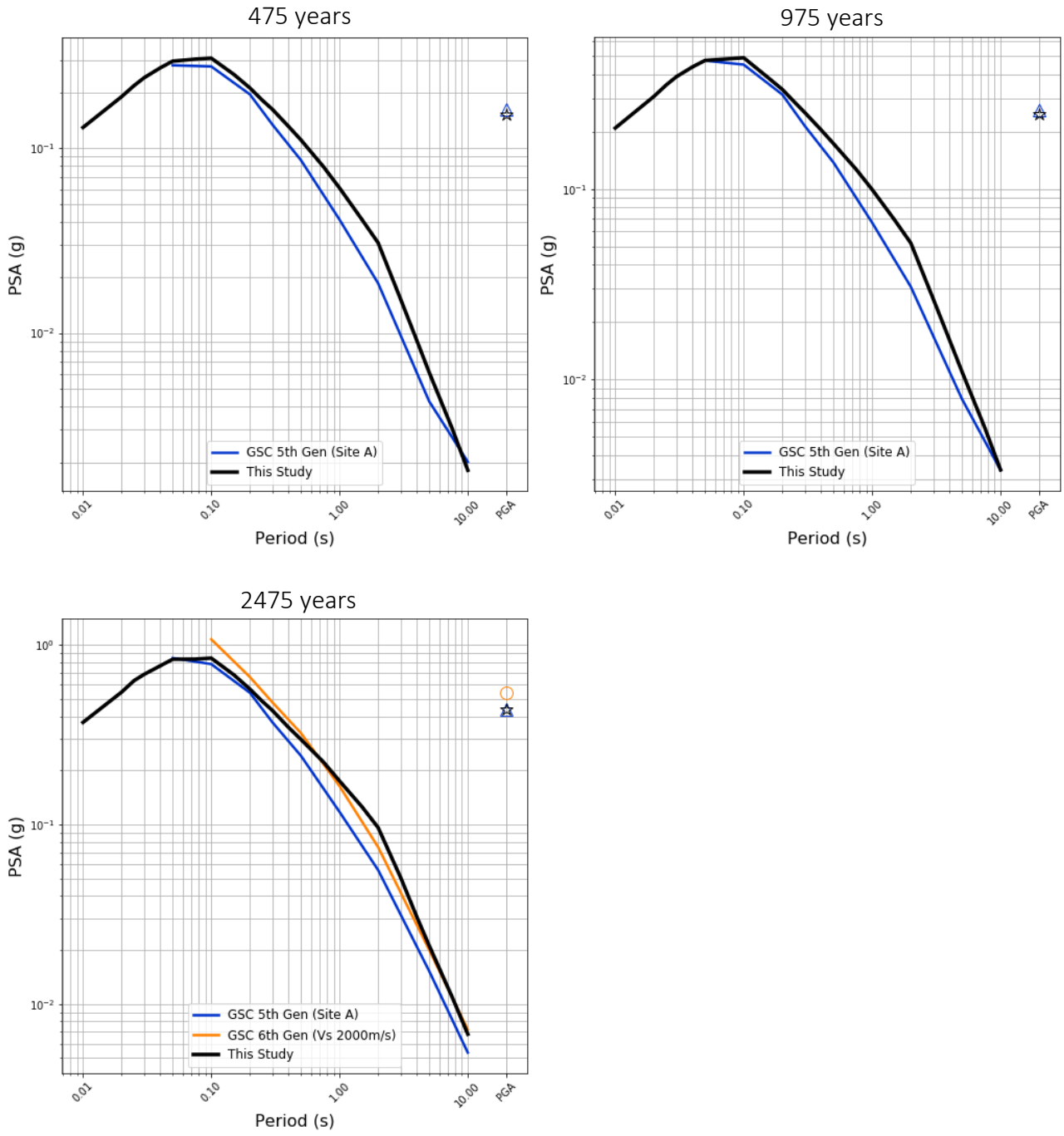

Figure 26. Horizontal-component uniform hazard spectra for hard rock condition (Class A) at the target site. The GSC's 5th and 6th generation hazard estimates for the target site are also shown, where available.

Vertical UHS are estimated from horizontal UHS by using published horizontal-to-vertical ratio (H/V) models. To verify which model is most appropriate, horizontal to vertical component ratios are calculated from seismograph recordings on bedrock stations within Saguenay, within Charlevoix, and at the closest station to the site, CHIQ (Figure 27). Siddiqqi and Atkinson (2002) studied the H/V spectra at bedrock seismograph stations across all of Canada, and assessed a subset of the national network stations in Eastern Canada. For eastern Canadian bedrock the horizontal components were found to be relatively unamplified at periods T > 1 s at a factor of 1.09. The amplification on horizontal components steadily increases to a constant factor of 1.48 as the period decreases to T = 0.2 s. Braganza and Atkinson (2016) studied the H/V spectra at 15 bedrock seismograph stations across Eastern Canada. The horizontal components were found to be relatively unamplified at periods T > 1 s. The amplification on horizontal components steadily increases to a constant factor of 1.2 as the period decreases to T = 0.1 s. The derived bedrock H/V amplification function of Braganza and Atkinson (2016) is very similar to the Canadian bedrock H/V determined by Siddiqqi and Atkinson (2002). Comparing the H/V values calculated empirically with published models, we find the Siddiqqi and Atkinson (2002) model for eastern Canadian bedrock is in relatively better agreement and is used to convert the horizontal UHS to the vertical UHS. The horizontal and vertical component UHS values as well as the Siddiqqi and Atkinson (2002) H/V ratios are provided in Table 3.

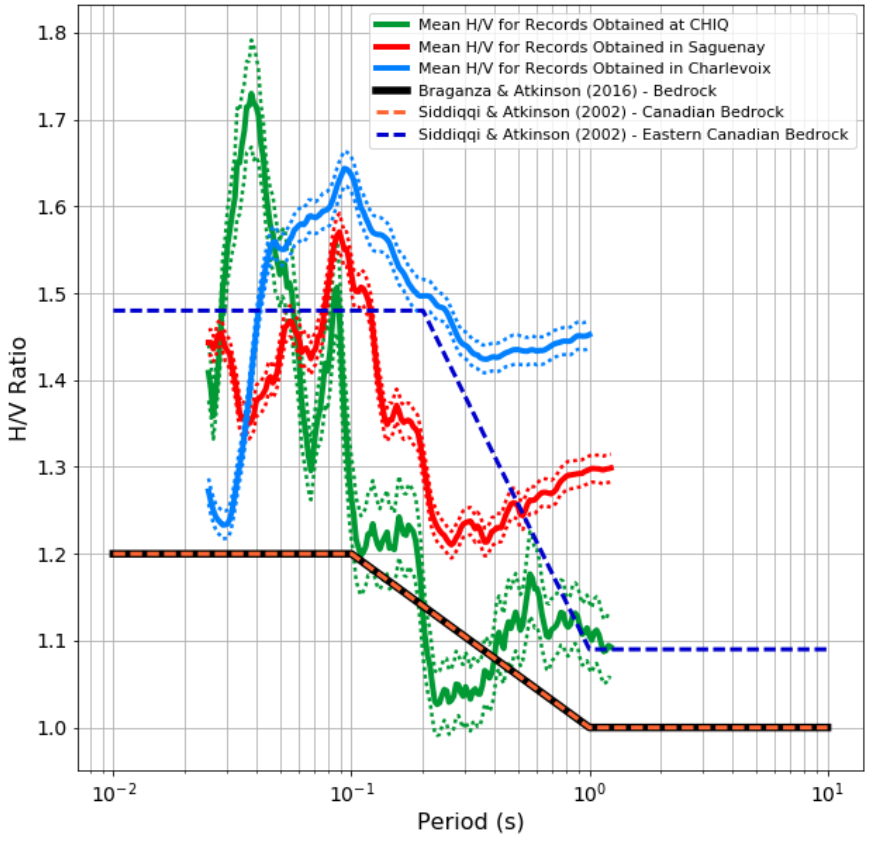

Figure 27. Horizontal to vertical (H/V) ratios computed from seismograph stations in Saguenay, Charlevoix and station CHIQ compared with bedrock models developed for rock sites in Canada.

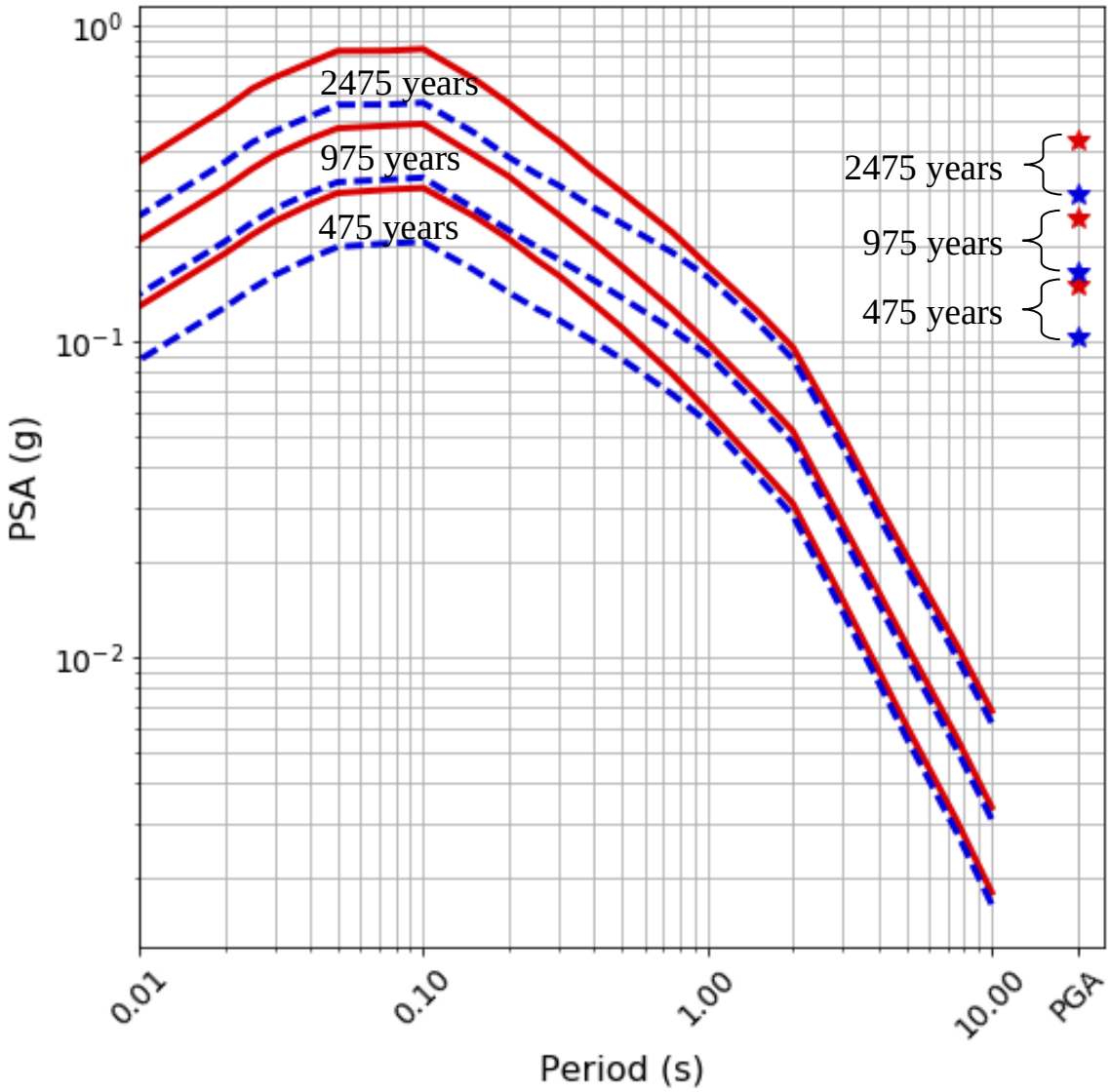

Figure 28. Comparison of horizontal (red) and vertical (blue) UHS determined for hard rock condition (Class A) at the target site for three return periods (475, 975 and 2475 years)

Hazard disaggregation assesses the relative contributions to the exceedance probability of a selected ground motion parameter over a range magnitudes (M) and distances (R). This enables to understand how different earthquake sources and magnitudes individually contribute to the rate of exceedance at the site. From these relative contributions, it is possible to identify earthquake scenarios that contribute most to the hazard for each response spectral period represented in the hazard analysis.

The contribution of event magnitudes and distances to the overall hazard at the target site are shown in Appendix A, B and C, for a subset of spectral periods. Hazard disaggregation for all periods considered in the analysis are provided in the electronic supplement to this report. The mean magnitude and distances for 475-year hazard is dominated by earthquakes at distances of

110 km (Charlevoix region) with magnitudes 6.0 < M < 6.5 across all periods. For the 975-year return period, contributions for short spectral periods (T < 0.1 s) become apparent at local distances (~30 km) with moderate magnitude earthquakes (5.5 < M < 6.0). At intermediate and long periods (T ≥ 0.1 s) the hazard becomes dominated by earthquakes of 6.0 < M < 7.0 from Charlevoix region. For the 2475-year return period, hazard at short and intermediate periods (T < 1 s) is dominated by 6.0 < M< 6.5 earthquakes in Saguenay area, where long period contributions come from 7.0 < M < 7.5 Charlevoix region. The mean and mode values of disaggregation with respect to magnitude and distance are shown in Tables 3, 4 and 5.

Table 2. Horizontal- and vertical-component UHS for hard rock condition (Class A) at the target site for 475, 975 and 2475 years return periods. Spectral and PGA values are in units of g. The Siddiqqi and Atkinson (2002) horizontal to vertical conversion factors are listed under SA02 H/V.

		Horizontal UHS			Vertical UHS		
Period (s)	SA02 H/V	475 years	975 years	2475 years	475 years	975 years	2475 years
0.01	1.48	1.29E-01	2.09E-01	3.70E-01	8.73E-02	1.41E-01	2.50E-01
0.02	1.48	1.90E-01	3.06E-01	5.45E-01	1.28E-01	2.07E-01	3.69E-01
0.03	1.48	2.40E-01	3.89E-01	6.85E-01	1.62E-01	2.63E-01	4.63E-01
0.05	1.48	2.95E-01	4.73E-01	8.31E-01	1.99E-01	3.20E-01	5.61E-01
0.1	1.48	3.06E-01	4.89E-01	8.43E-01	2.07E-01	3.30E-01	5.70E-01
0.2	1.48	2.12E-01	3.33E-01	5.67E-01	1.43E-01	2.25E-01	3.83E-01
0.3	1.38	1.62E-01	2.52E-01	4.31E-01	1.17E-01	1.82E-01	3.12E-01
0.5	1.26	1.11E-01	1.73E-01	2.97E-01	8.80E-02	1.38E-01	2.36E-01
1	1.09	6.08E-02	9.95E-02	1.75E-01	5.58E-02	9.13E-02	1.60E-01
2	1.09	3.07E-02	5.21E-02	9.60E-02	2.82E-02	4.78E-02	8.81E-02
5	1.09	6.12E-03	1.10E-02	2.11E-02	5.62E-03	1.01E-02	1.94E-02
10	1.09	1.81E-03	3.36E-03	6.79E-03	1.66E-03	3.09E-03	6.23E-03
PGA	1.48	1.52E-01	2.46E-01	4.34E-01	1.03E-01	1.66E-01	2.93E-01

Table 3. Hazard disaggregation for 475-year return period

T (s)	Magnitude		Distance (km)	
	Mean	Mode	Mean	Mode
0.01	6.2	6.3	82.5	110.0
0.02	6.1	6.5	79.4	110.0
0.03	6.1	6.5	78.7	110.0
0.05	6.1	6.5	77.5	110.0
0.1	6.2	6.5	81.5	110.0
0.2	6.3	6.3	91.6	110.0
0.3	6.3	6.3	101.6	110.0
0.5	6.4	6.5	119.8	110.0
1	6.5	6.5	140.2	110.0
2	6.6	6.5	160.0	110.0
5	6.7	6.5	172.6	110.0
10	6.7	6.5	178.8	110.0
PGA	6.2	6.5	80.7	110.0

Table 4. Hazard disaggregation for 975-year return period

T (s)	Magnitude		Distance (km)	
	Mean	Mode	Mean	Mode
0.01	6.3	5.5	70.0	30.0
0.02	6.3	5.7	67.5	30.0
0.03	6.3	5.7	67.2	30.0
0.05	6.3	5.7	66.0	30.0
0.1	6.4	6.7	69.4	110.0
0.2	6.4	6.5	77.8	110.0
0.3	6.5	6.7	86.5	110.0
0.5	6.6	6.7	101.7	110.0
1	6.7	6.7	120.6	110.0
2	6.8	6.7	140.5	110.0
5	6.9	6.7	156.7	110.0
10	6.9	6.7	166.0	110.0
PGA	6.3	5.7	68.3	30.0

Table 5. Hazard disaggregation for 2475-year return period

T (s)	Magnitude		Distance (km)	
	Mean	Mode	Mean	Mode
0.01	6.5	6.3	56.6	30.0
0.02	6.5	6.5	55.4	30.0
0.03	6.5	6.3	54.4	30.0
0.05	6.5	6.1	53.5	30.0
0.1	6.5	6.5	56.1	30.0
0.2	6.6	6.3	63.3	30.0
0.3	6.7	6.3	70.0	30.0
0.5	6.8	6.5	82.5	30.0
1	6.9	6.7	97.7	110.0
2	7.0	7.3	116.3	110.0
5	7.1	7.3	134.5	110.0
10	7.1	7.3	148.1	110.0
PGA	6.5	6.3	54.4	30.0

8. Summary

A site-specific PSHA is conducted for a site of a proposed liquid natural gas facility near Saguenay, Québec. The 5th generation hazard model of GSC is refined with focus on the potential seismicity and their ground motions in the site vicinity. The source zones and magnitude recurrence models of GSC are checked for applicability based on the observed seismicity patterns as well as potential characteristic earthquakes on postulated faults in the study area. Two alternative suites of ground motion models are developed to provide a link between earthquake occurrences and potential ground motions at the site. The probability of exceeding a specified level of ground motion at the site is calculated by summing up the hazard contributions over all magnitudes and distances, including sources within 500 km of the site. The EqHaz software package (Assatourians and Atkinson, 2013) is used for the analysis.

Hazard calculations are performed for PGA and 5%-damped PSA between 0.01 s ≤ T ≤ 10 s, for three return periods: 475, 975 and 2475 years. Hard rock site uniform hazard spectra are determined for horizontal and vertical components (Table 2). Hazard disaggregation analysis indicates that for the 475-year return period the hazard is controlled by moderate magnitude earthquakes in the Charlevoix area. For the 975- and 2475-year return periods, moderate magnitude earthquakes within the Saguenay region begin to dominate short-to-intermediate periods, whereas long periods are controlled by large magnitude earthquakes in the Charlevoix area.

9. References

Abrahamson, N., and J. Bommer (2005). Probability and uncertainty in seismic hazard analysis, *Earthquake Spectra*, 21: 603-608.

Adams, J., and P. Basham (1989). The seismicity and seismotectonics of Canada east of the Cordillera, *Geoscience Canada*, 16: 3–16.

Adams, J., and P. Basham (1991). The seismicity and seismotectonics of eastern Canada, *The Geology of North America*, Decade Map Volume 1: 261-276.

Adams, J. and S. Halchuk (2003). Fourth generation seismic hazard maps of Canada: values for over 650 Canadian localities intended for the 2005 National Building Code of Canada; Geological Survey of Canada, Open File 4459, 2003, 155 pages, https://doi.org/10.4095/214223

Adams, J., S. Halchuk, T. Allen, and G. Rogers (2015). Canada's 5th generation seismic hazard model, as prepared for the 2015 National Building Code of Canada, *11th Canadian Conference on Earthquake Engineering*, Paper 93775.

Adams, J., T. Allen, S. Halchuk, and M. Kolaj (2019). Canada's 6th generation seismic hazard model, as prepared for the 2020 national building code of Canada, *12th Can. Conf. Earthquake Engineering, Quebec City*, 192-Mkvp-139.

Anderson, J., and J. Brune (1999). Methodology for using precarious rocks in Nevada to test seismic hazard models, *Bulletin of the Seismological Society of America*, 89: 456-467.

Anderson, J., J. Brune, R. Anooshehpoor, and S. Ni (2000). New ground motion data and concepts in seismic hazard analysis, *Current Science*, 79: 1278–1290.

Assatourians, K., and G. M. Atkinson (2013). EqHaz: An open-source probabilistic seismic-hazard code based on the Monte Carlo simulation approach, *Seismological Research Letters*, 84: 516-524.

Assatourians, K., and G. M. Atkinson (2019). Implementation of a smoothed-seismicity algorithm in Monte Carlo PSHA software EqHaz and implications for localization of hazard in the Western Canada Sedimentary Basin, *Seismological Research Letters*, 90: 1407–1419

Atkinson, G. M. (2006). Single-station sigma. *Bulletin of the Seismological Society of America*, 96: 446–455.

Atkinson, G. M. (2011). An empirical perspective on uncertainty in earthquake ground motions, *Canadian Journal of Civil Engineering*, 38: 1002–1015.

Atkinson, G. M. (2013). Empirical evaluation of aleatory and epistemic uncertainty in eastern ground motions, *Seismological Research Letters*, 84: 130–138.

Atkinson, G. M., and J. Adams (2013). Ground motion prediction equations for application to the 2015 Canadian national seismic hazard maps, *Canadian Journal of Civil Engineering*, 40: 988-998.

Atkinson, G. M., and K. Goda (2011). Effects of seismicity models and new ground-motion prediction equations on seismic hazard assessment for four Canadian cities, *Bulletin of the Seismological Society of America*, 101: 176–189.

Atkinson, G. M., J. J. Bommer, and N. A. Abrahamson (2014). Alternative approaches to modeling epistemic uncertainty in ground motions in probabilistic seismic-hazard analysis, *Seismological Research Letters*, 85: 1141-1144.

Atkinson, G. M., B. Hassani, A. Singh, E. Yenier, and K. Assatourians (2015). Estimation of moment magnitude and stress parameter from ShakeMap ground-motion parameters, *Bulletin of the Seismological Society of America*, 105: 2572–2588.

Baird, A. F., S. D. McKinnon, and L. Godin (2009). Stress channelling and partitioning of seismicity in the Charlevoix seismic zone, Quebec, Canada, *Geophysical Journal International*, 179: 559–568.

Baird, A. F., S. D. McKinnon, and L. Godin (2010). Relationship between structures, stress and seismicity in the Charlevoix seismic zone revealed by 3-D geomechanical models: implications for the seismotectonics of continental interiors. *Journal of Geophysical Research*, 115: 2156–2202.

Bent, A.L. & Perry, H.K.C., 2003. Focal Mechanisms for Eastern Canadian Earthquakes, 1994 - 2000, Seism. Res. Let., 74, 452–468, doi:1785/gssrl.74.4.452.

Boore, D. M., and G. M. Atkinson (1992). Source spectra for the 1988 Saguenay, Quebec, earthquakes, *Bulletin of the Seismological Society of America*, 82: 683–719.

Braganza, S., G. M. Atkinson, H. Ghofrani, B. Hassani, L. Chouinard, P. Rosset, D. Motazedian, J. Hunter (2016). Modeling site amplification in Eastern Canada on a regional scale, *Seismological Research Letters*, 87: 1008–1021.

Budnitz, R. J., G. Apostolakis, D. M. Boore, L. S. Cluff, K. J. Coppersmith, C. A. Cornell, and P. A. Morris (1997). *Recommendations for probabilistic seismic hazard analysis: Guidance on uncertainty and use of experts*, NUREG/CR-6372, Two volumes, U.S. Nuclear Regulatory Commission, Washington, D.C.

Cornell, C. (1968). Engineering seismic risk analysis. *Bulletin of the Seismological Society of America*, 58: 1583-1606.

Crone, A. J., P. M. De Martini, M. N. Cachette, K. Okumura, and J. R. Prescott (2003). Paleoseismicity of two historically quiescent faults in Australia: Implications for fault behavior in stable continental regions, *Bulletin of the Seismological Society of America*, 93: 1913–1934.

Crough, S. T. (1981). Mesozoic hot spot epeirogeny in eastern North America. Geology, 9: 2–6.

CAN/CSA-Z276-18 (2018). Liquefied natural gas (LNG) - Production, storage, and handling, *CSA Group*, 214 pp.

Du Berger, R., D. W. Roy, M. Lamontagne, G. Woussen, R. G. North, R. J. Wetmiller (1991). The Saguenay (Quebec) earthquake of November 25, 1988: seismologic data and geologic setting, *Tectonophysics*, 186: 59-74.

Ebel, J. E. (1984). Statistical aspects of New England Seismicity from 1975 to 1982 and implications for past and future earthquake activity, *Bulletin of the Seismological Society of America*, 74: 1311-1329.

Faure, S., A. Tremblay, and J. Angelier (1996), Alleghanian paleostress reconstruction in the northern Appalachians: Intraplate deformation between Laurentia and Gondwana, *Geol. Soc. Am. Bull.*, 108: 1467– 1480.

Goulet, C., B. Yousef, N. Abrahamson, N. Kuehn, L. Al Atik, R. Youngs, and R. Graves (2018). Central and eastern North America ground-motion characterization - NGA-East final report, *Pacific Earthquake Engineering Research Center*, PEER 2018/08, 817 pp.

Halchuk, S. C., J. E. Adams, and T. I. Allen (2015). Fifth generation seismic hazard model for Canada: Grid values of mean hazard to be used with the 2015 National Building Code of Canada, Geological Survey of Canada, Open File 7893.

Halchuk, S. C., T. I. Allen, G. C. Rogers, and J. Adams (2015). Seismic Hazard Earthquake Epicentre File (SHEEF2010) used in the Fifth Generation Seismic Hazard Maps of Canada, *Geological Survey of Canada*, Open File 7724, 21 pp.

Johnston, A., K. Coppersmith, L. Kanter, and C. Cornell (1994). The earthquakes of stable continental regions, *Electric Power Research Institute*, Report TR-102261-V1

Kolaj, M., T. Allen, R. Mayfield, J. Adams, and S. Halchuk (2019). Ground-motion models for the 6th Generation Seismic Hazard Model of Canada, *12th Can. Conf. Earthquake Engineering, Quebec City*, 192-hHtH-159.

Kolaj, M., S. Halchuk, J. Adams, and T. I. Allen (2020). Trial Sixth Generation seismic-hazard model of Canada: seismic-hazard values for selected localities, Geological Survey of Canada, Open File 8629.

Kumarapeli, P. S. (1985). Vestiges of Iapetan rifting in the west of the northern Appalachians. *Geoscience Canada*, 12: 54–59.

Lamontagne, M. (1987). Composite P-nodal solution analysis of earthquakes from the Charlevoix seismic zone, *Canadian Journal of Earth Sciences*, 24: 2118-2129.

Lamontagne, M. (1999). Rheological and geological constraints on the earthquake distribution in the Charlevoix Seismic Zone, Quebec, Canada, PhD Thesis, Carleton University, 386 pp.

Lamontagne, M., Halchuk, S., Cassidy, J. F., and Rogers, G. C. (2008a). Significant Canadian earthquakes of the period 1600–2006. Seismological Research Letters, 79, 211–223.

Lamontagne, M., and G. Ranalli (2014). Earthquakes and geological structures of the St. Lawrence Rift System, *Intraplate Earthquakes*, Cambridge University Press.

Lemieux, Y., A. Tremblay, and D. Lavois (2003), Structural analysis of supracrustal faults in the Charlevoix area, Que´bec: Relation to impact cratering and the St-Laurent fault system, *Canadian Journal of Earth Sciences*, 40: 221–235.

Leonard, M., D. R. Burbidge, T. I. Allen, D. J. Robinson, A. McPherson, D. Clark, and C. D. N. Collins (2014). The challenges of probabilistic seismic-hazard assessment in stable continental interiors: An Australian example, *Bulletin of the Seismological Society of America*, 104: 3008-3028.

Llenos, A. L., and A. J. Michael (2020) Regionally optimized background earthquake rates from ETAS (ROBERE) for probabilistic seismic hazard assessment, *Bulletin of the Seismological Society of America*, 110 (in press).

Locat, Jacques & Martin, F. & Levesque, Christiane & Locat, P. & Leroueil, Serge & Konrad, Jean-Marie & Urgeles, Roger & Canals, Miquel & Duchesne, Mathieu. (2003). Submarine Mass Movements In The Upper Saguenay Fjord, (Québec, Canada), Triggered by the 1663 Earthquake. Submarine Mass Movements and their Consequences. 10.1007/978-94-010-0093-2_56.

Locat, Jacques & Levesque, Christiane. (2009). The Saquency Fjord: A unique physiography and records. Revue des Sciences de l'Eau. 22. 135-157.

Locat, Jacques. (2011). Localization and magnitude of seismicity on February 5 1663 (Charlevoix) in landslide journals. Canadian Geotechnical Journal. 48. 1266-1286.

Ma, S., Motazedian, D., Lamontagne, M. (2018), Further studies on the 1988 MW 5.9 Saguenay, Quebec, earthquake sequence, Canadian Journal of Earth Sciences, 2018, 55(10): 1115-1128, https://doi.org/10.1139/cjes-2017-0231

Mazzotti, S., T. S. James, J. Henton, and J. Adams (2005). GPS crustal strain, postglacial rebound, and seismic hazard in eastern North America: The Saint Lawrence valley example, *Journal of Geophysical Research*, 110: B11301.

Mazzotti, S., J. Townend (2010). State of stress in central and eastern North American seismic zones, *Lithosphere*, 2: 76–83.

McGuire, R. (1976). FORTRAN computer program for seismic risk analysis, *U.S. Geological Survey*, Open-file report. 76-67.

McGuire, R. (1977). Seismic design spectra and mapping procedures using hazard analysis based directly on oscillator response. *International Journal of Earthquake Engineering and Structural Dynamics*, 5: 211-234.

McGuire, R. (2004). Seismic hazard and risk analysis, EERI Monograph MNO-10. *Earthquake Engineering Research Institute*, Oakland, California.

Munro, P. S., and North, R. G. (1989) The Saguenay Earthquake of November 25, 1988, Strong Motion Data / Le Tremblement De Terre Du Saguenay, Le 25 Novembre 1988, Enregistrements Des Secousses Fortes, Geological Survey of Canada, Open File 1976, 1989, 16 pages, https://doi.org/10.4095/130579

NBCC (2015). *National Building Code of Canada*, National Research Council of Canada, Volume 1, 1412 pp.

Palmer, S., and G. M. Atkinson (2020). The High-frequency decay slope of spectra (kappa) for M≥3.5 earthquakes on rock sites in Eastern and Western Canada, *Bulletin of the Seismological Society of America,* 110: 471–488.

Rondot, J. (1968). Nouvel impact meteoritique fossile? La structure semicirculaire de Charlevoix, *Canadian Journal of Earth Sciences*, 5: 1305– 1317.

Siddiqqi J., and G. M. Atkinson (2002). Ground-motion amplification at rock sites across Canada as determined from horizontal-vertical component ratio, *Bulletin of the Seismological Society of America*, 92: 877–884.

Stein, S., and M. Liu (2009). Long aftershock sequences within continents and implications for earthquake hazard assessment, *Nature*, 462: 87-89.

Stein, S., M. Liu, E. Calais, and Q. Li (2009). Mid-continent earthquakes as a complex system, *Seismological Research Letters*, 80, 551–553.

Strasser, F., N. Abrahamson, and J. Bommer (2009). Sigma: Issues, insights and challenges, *Seismological Research Letters*, 80: 40–56.

Swafford, L., and S. Stein (2007). Limitations of the short earthquake record for seismicity and seismic hazard studies, *Geological Society of America Special Papers*, 425: 49.

Sykes, L. (1978). Intraplate seismicity, reactivation of preexisting zones of weakness, alkaline magmatism, and other tectonism postdating continental fragmentation, *Reviews of Geophysics*, 16: 621–688.

Tremblay, A., and M. K. Roden-Tice (2011). Iapetan versus Atlantic rifting history of Laurentia: constraints from field mapping and AFT dating of Precambrian basement rocks, Canada. *Geological Society of America*, 42: 79.

Tremblay, A., M. K. Roden-Tice, J. A. Brandt, and T. W. Megan (2013). Mesozoic fault reactivation along the St. Lawrence rift system, eastern Canada: Thermochronologic evidence from apatite fission-track dating, *Geological Society of America Bulletin*, 125: 794–810.

Turmel, Dominique & Locat, Jacques. (2016). Location of the 1663 earthquake epicenter by the simulation of seismic wave propagation at a regional scale. 10.1201/b21520-241.

Tuttle, M. P., and G. M. Atkinson (2010). Localization of Large Earthquakes in the Charlevoix Seismic Zone, Quebec, Canada, during the Past 10,000 Years, *Seismological Research Letters*, 81: 140-147.

Williams, H. (1979), Appalachian orogen in Canada, *Canadian Journal of Earth Sciences*, 16:792–807.

Yenier, E. and G. M. Atkinson (2015). Regionally adjustable generic ground-motion prediction equation based on equivalent point-source simulations: application to Central and Eastern North America, *Bulletin of the Seismological Society of America*, 105: 1989–2009.

Appendix A Hazard disaggregation for 475-year return period

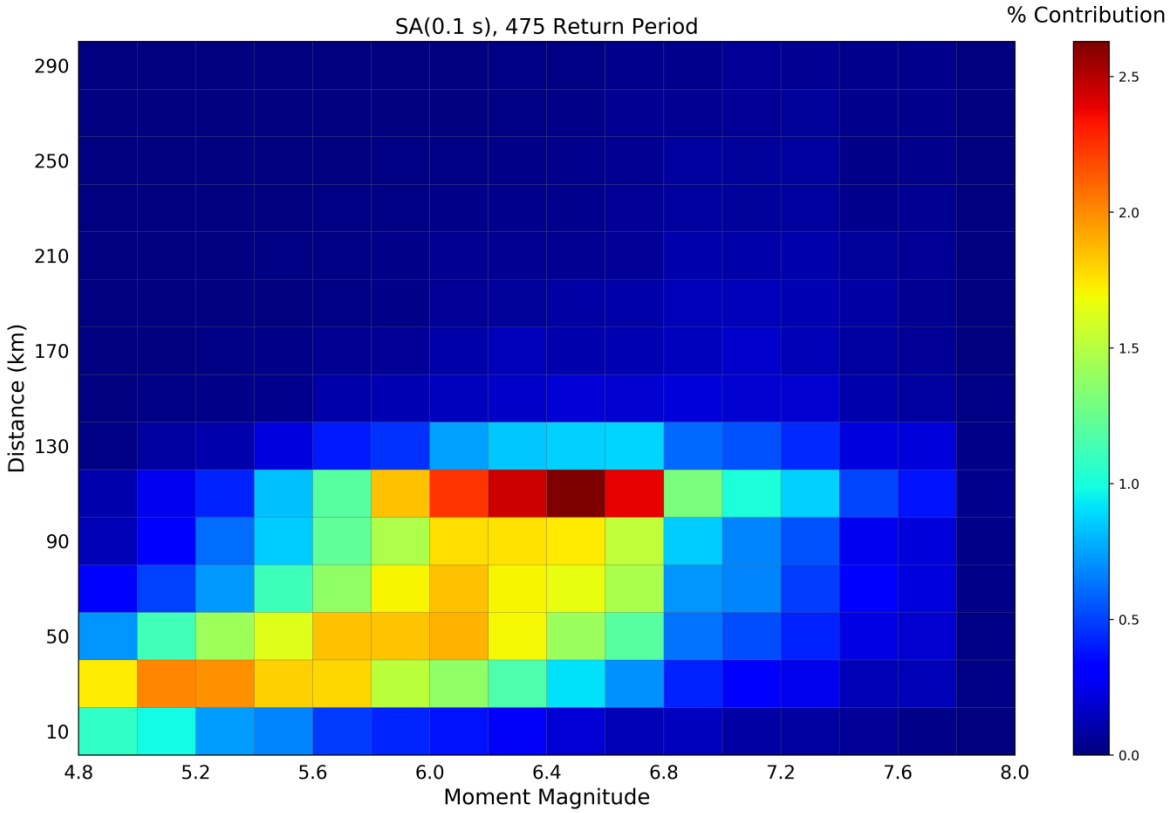

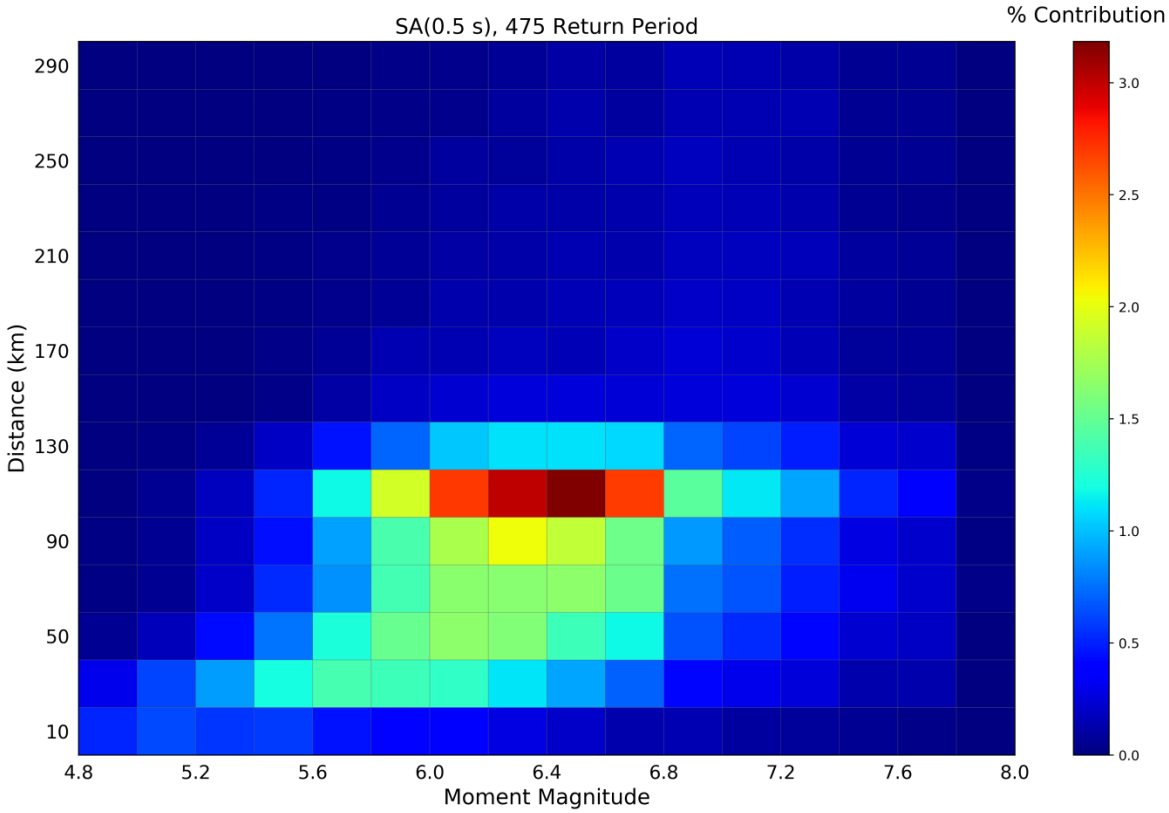

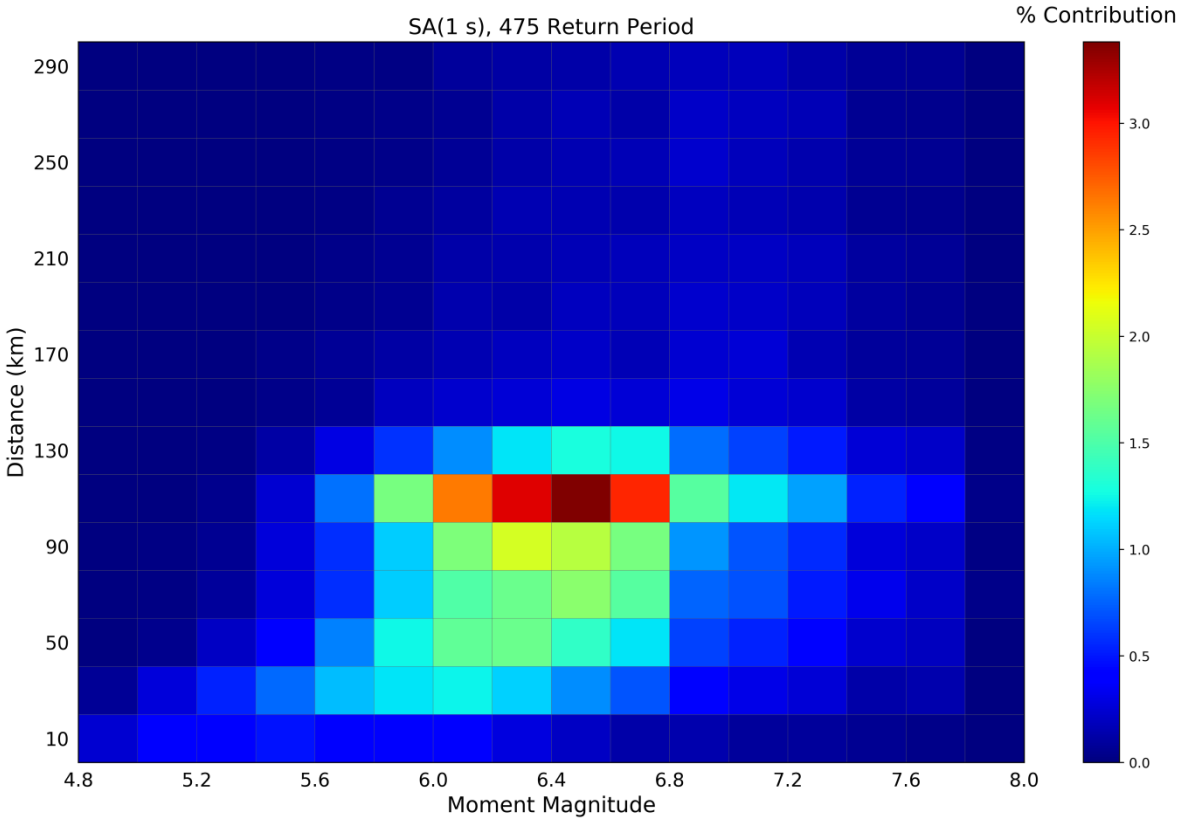
SA(1 s), 475 Return Period
% Contribution
Distance (km)
290
250
210
170
130
90
50
10
4.8
5.2
5.6
6.0
6.4
6.8
7.2
7.6
8.0
Moment Magnitude
3.0
2.5
2.0
1.5
1.0
0.5
0.0

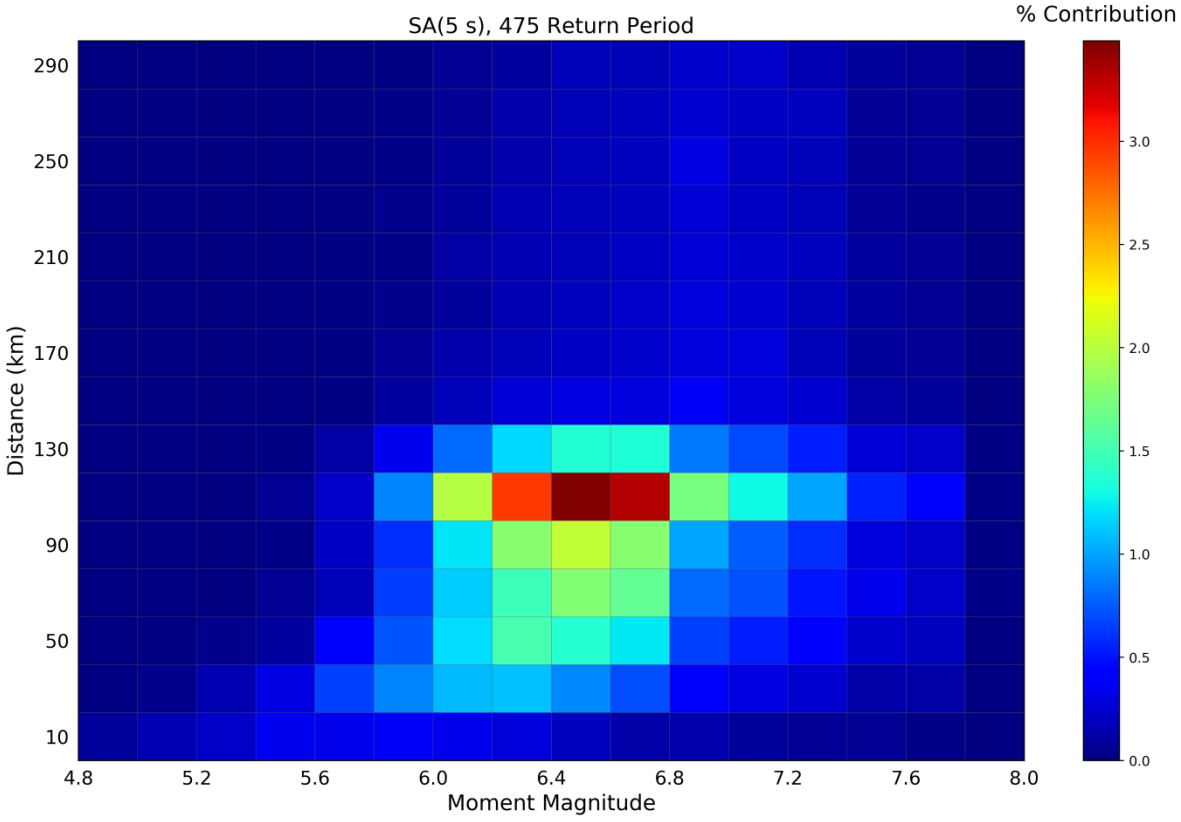
SA(5 s), 475 Return Period
% Contribution
Distance (km)
290
250
210
170
130
90
50
10
4.8
5.2
5.6
6.0
6.4
6.8
7.2
7.6
8.0
Moment Magnitude
3.0
2.5
2.0
1.5
1.0
0.5
0.0

Appendix B Hazard disaggregation for 975-year return period

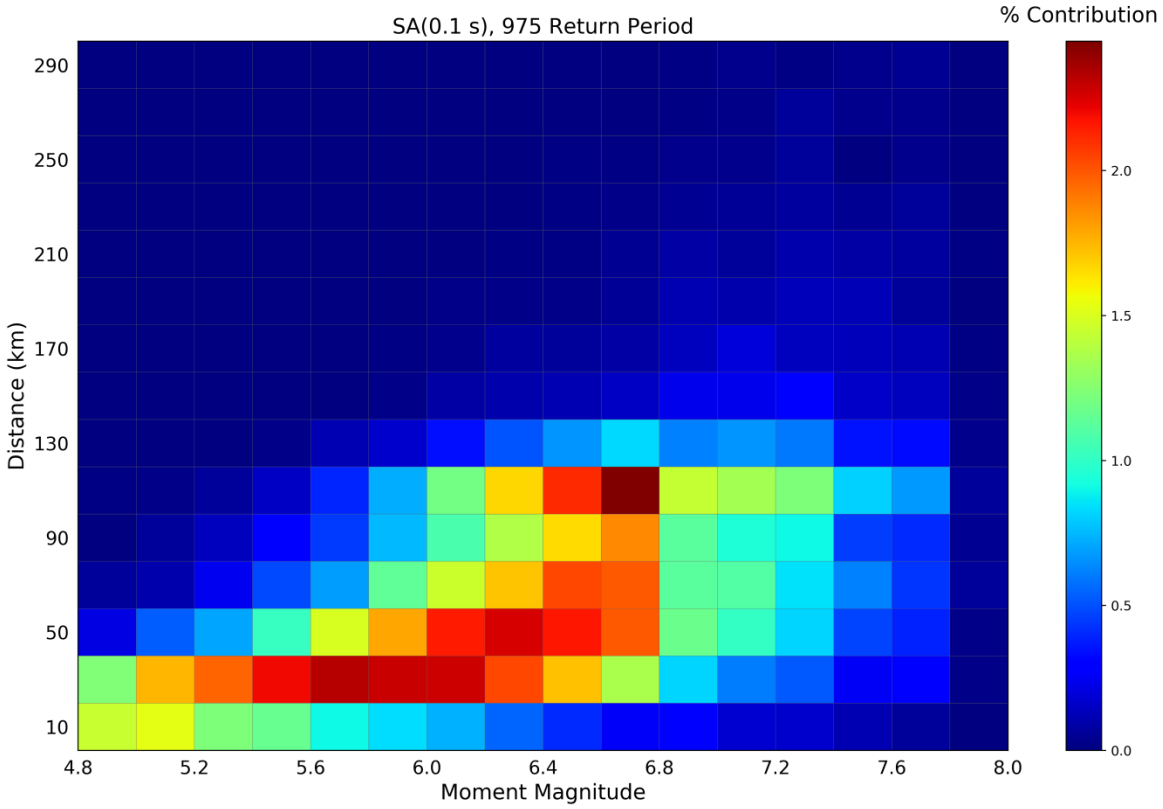

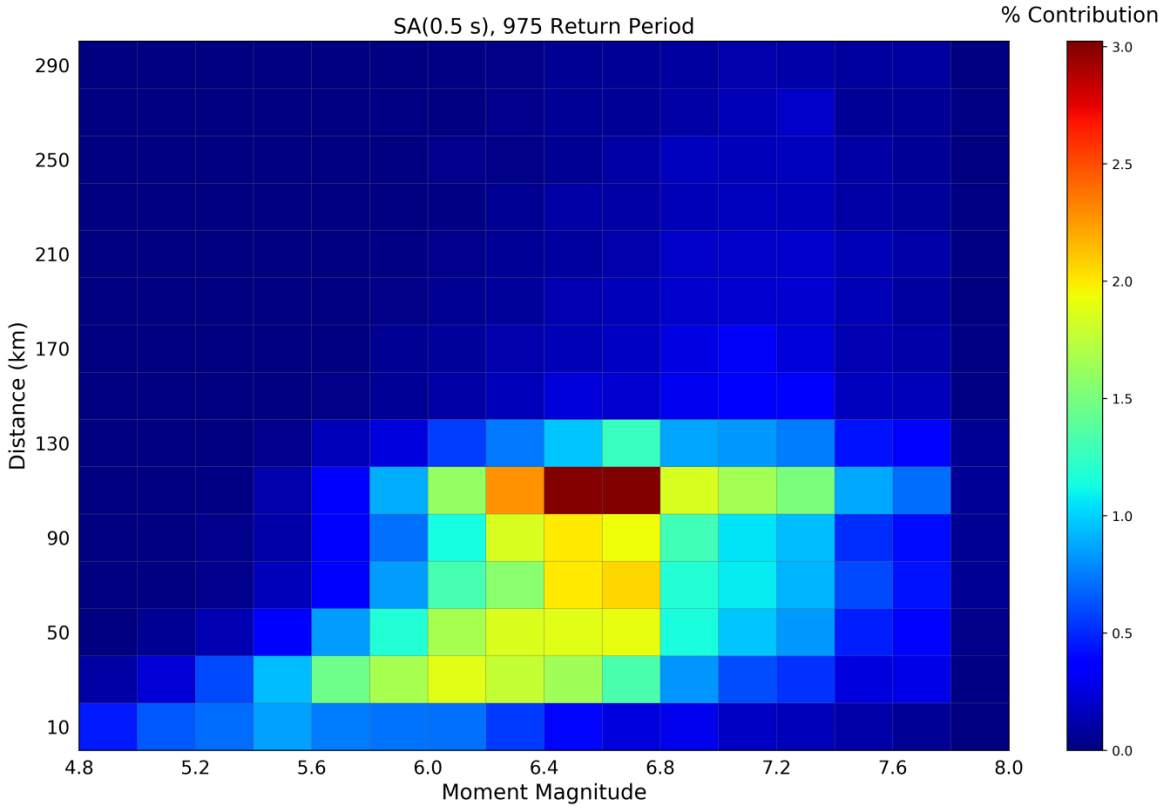

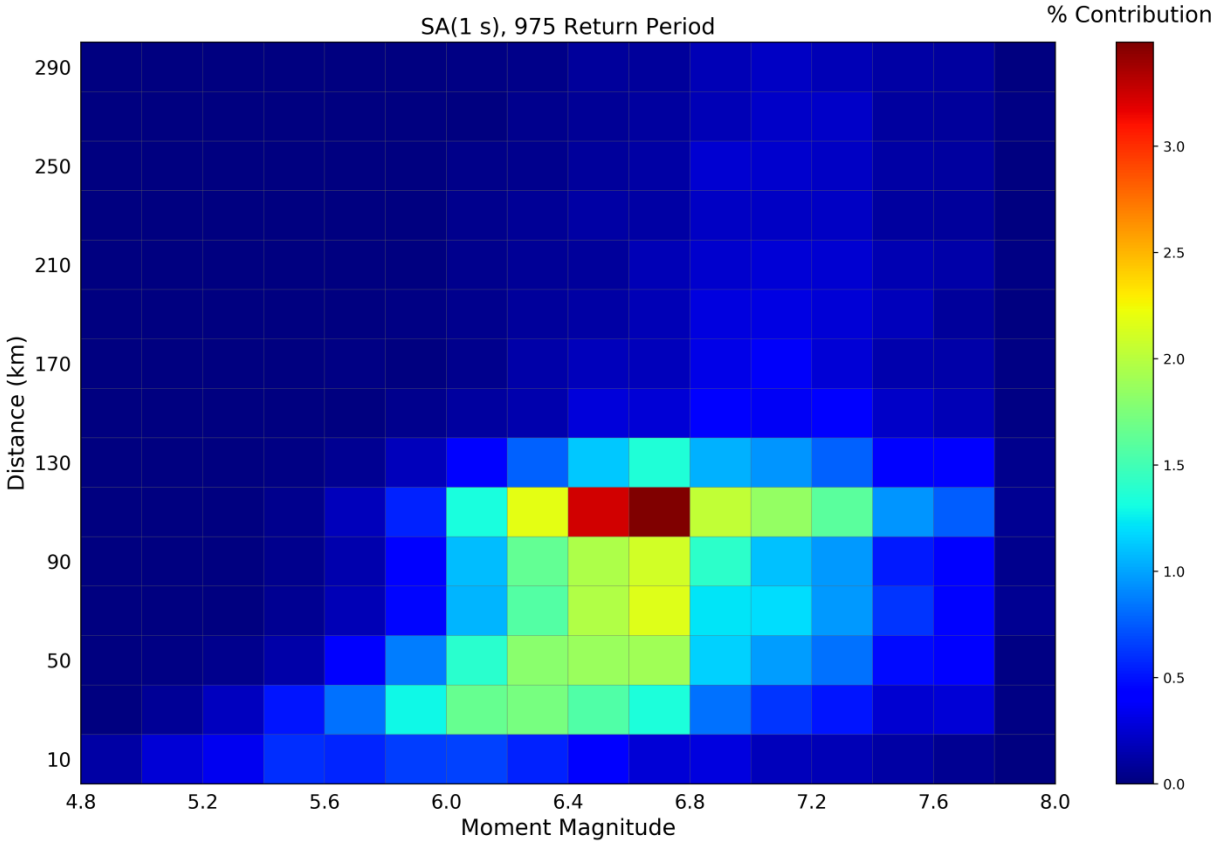
SA(1 s), 975 Return Period
% Contribution
Distance (km)
290
250
210
170
130
90
50
10
4.8
5.2
5.6
6.0
6.4
6.8
7.2
7.6
8.0
Moment Magnitude
3.0
2.5
2.0
1.5
1.0
0.5
0.0

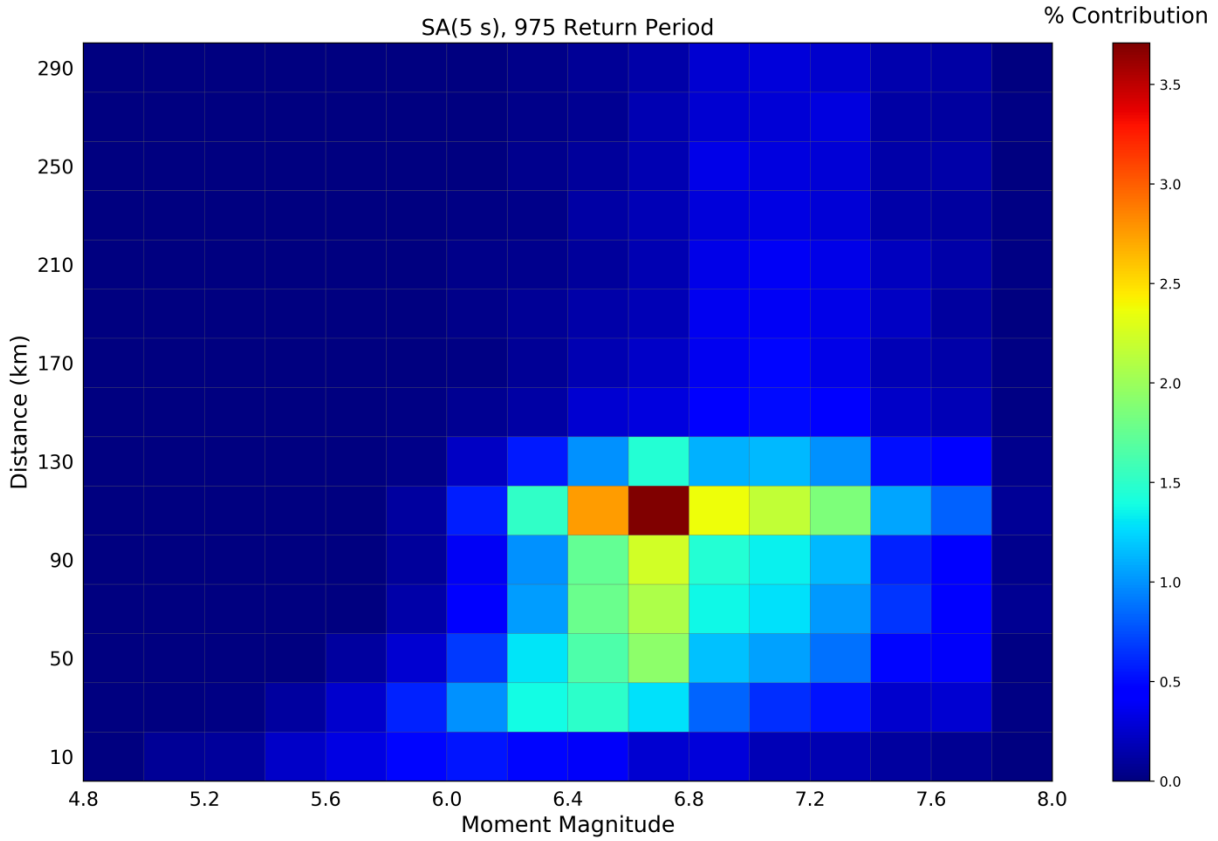
SA(5 s), 975 Return Period
% Contribution
Distance (km)
290
250
210
170
130
90
50
10
4.8
5.2
5.6
6.0
6.4
6.8
7.2
7.6
8.0
Moment Magnitude
3.5
3.0
2.5
2.0
1.5
1.0
0.5
0.0

Appendix C Hazard disaggregation for 2475-year return period

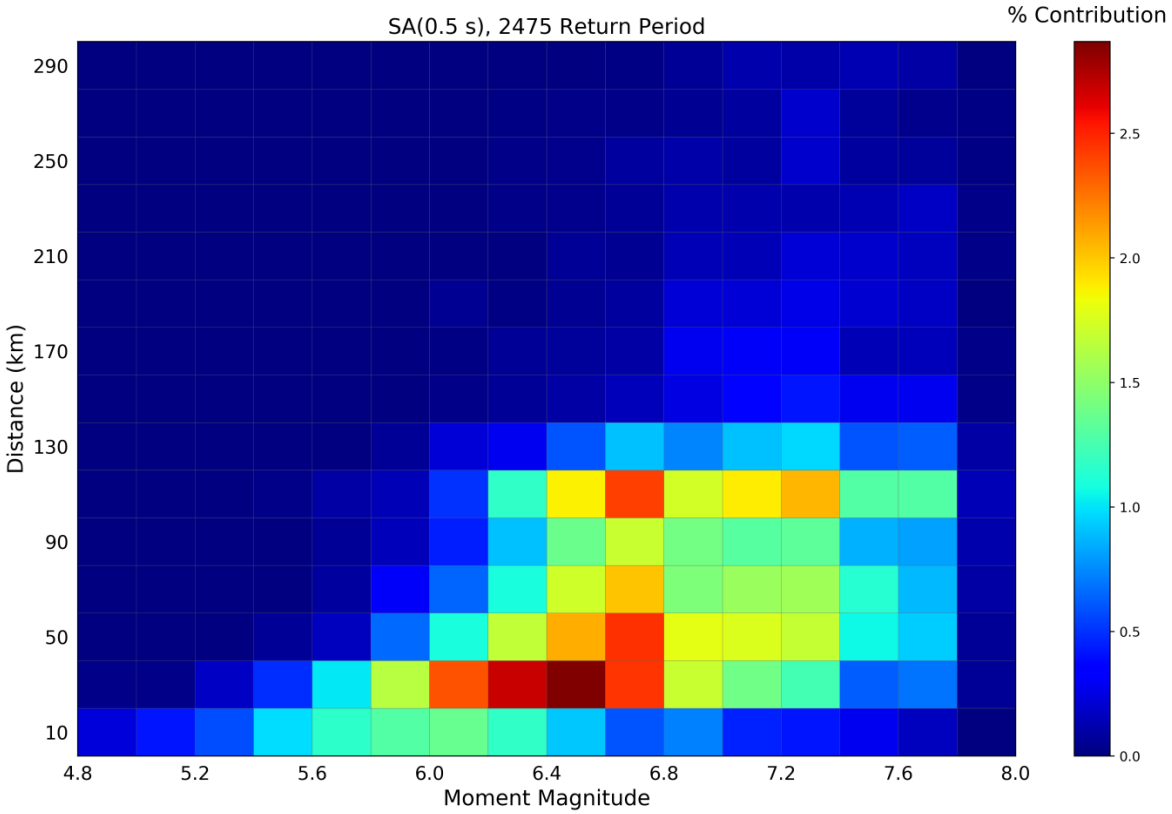

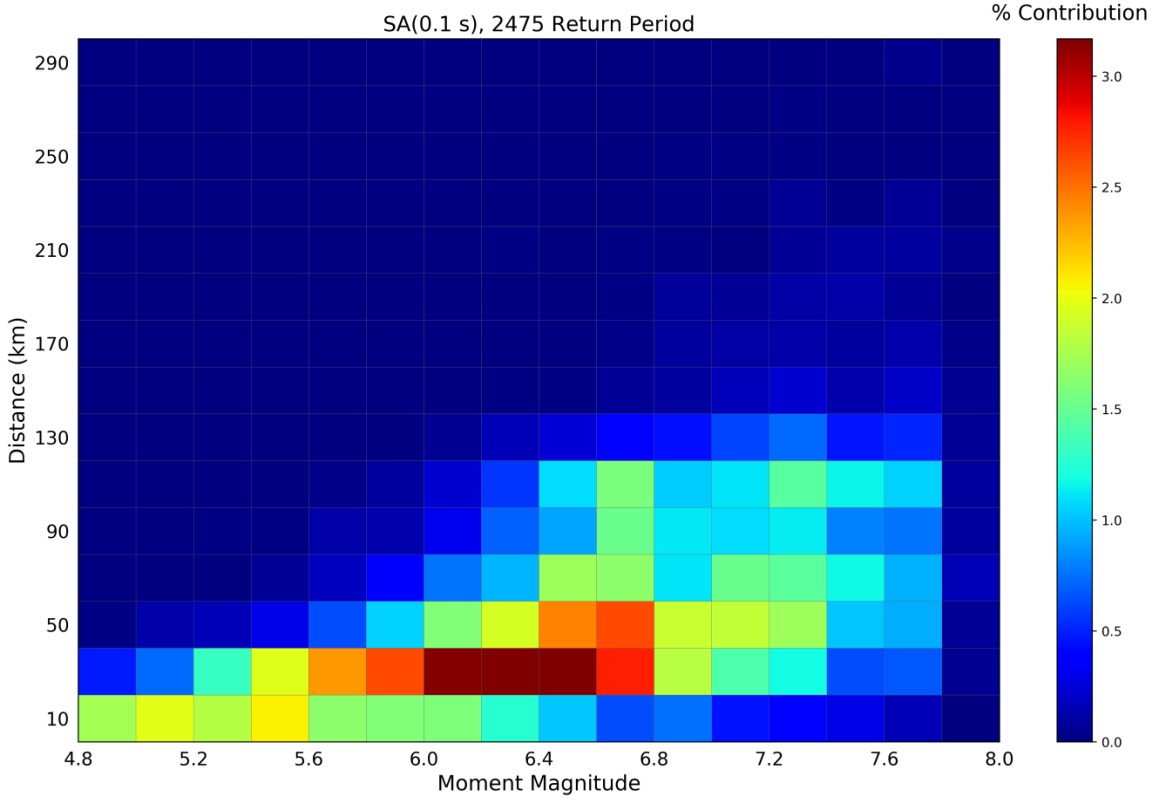

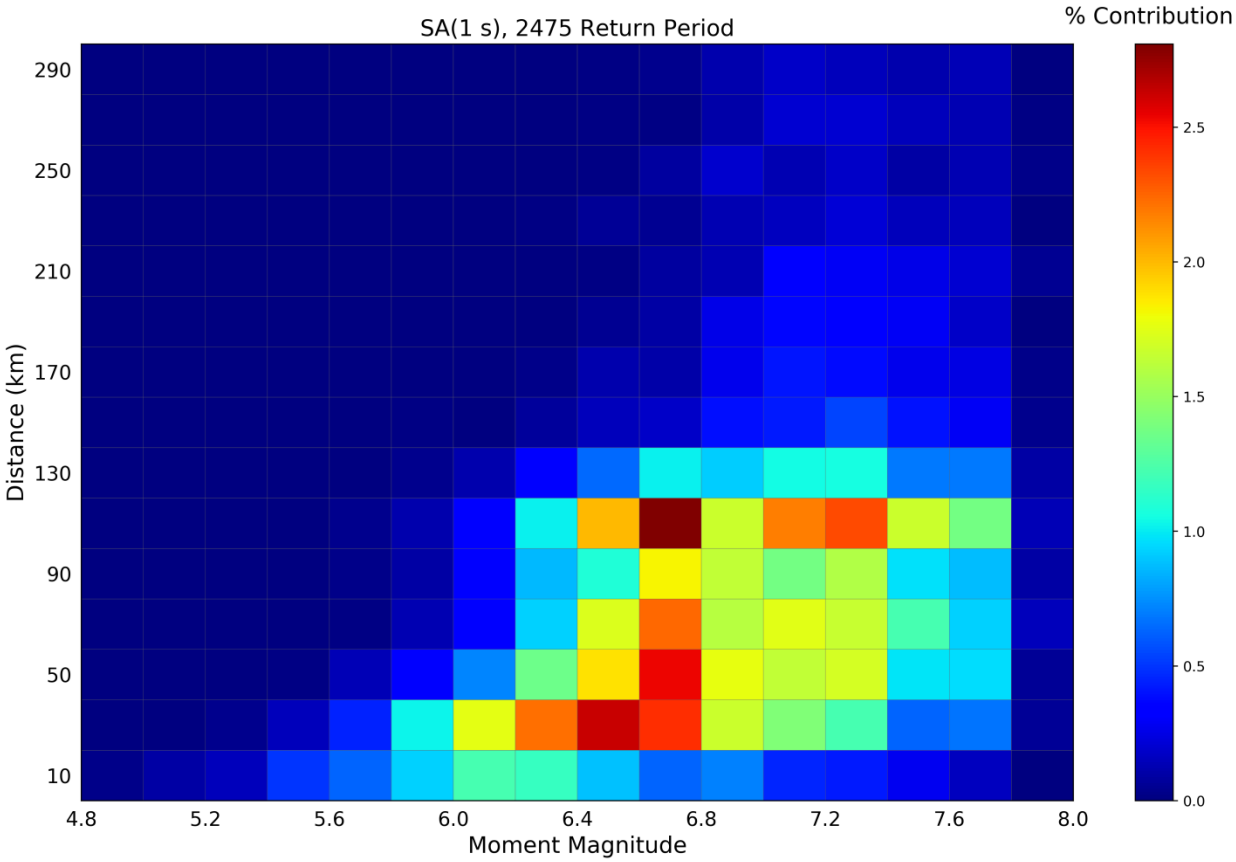
SA(1 s), 2475 Return Period
% Contribution
Distance (km)
290
250
210
170
130
90
50
10
4.8
5.2
5.6
6.0
6.4
6.8
7.2
7.6
8.0
Moment Magnitude
2.5
2.0
1.5
1.0
0.5
0.0

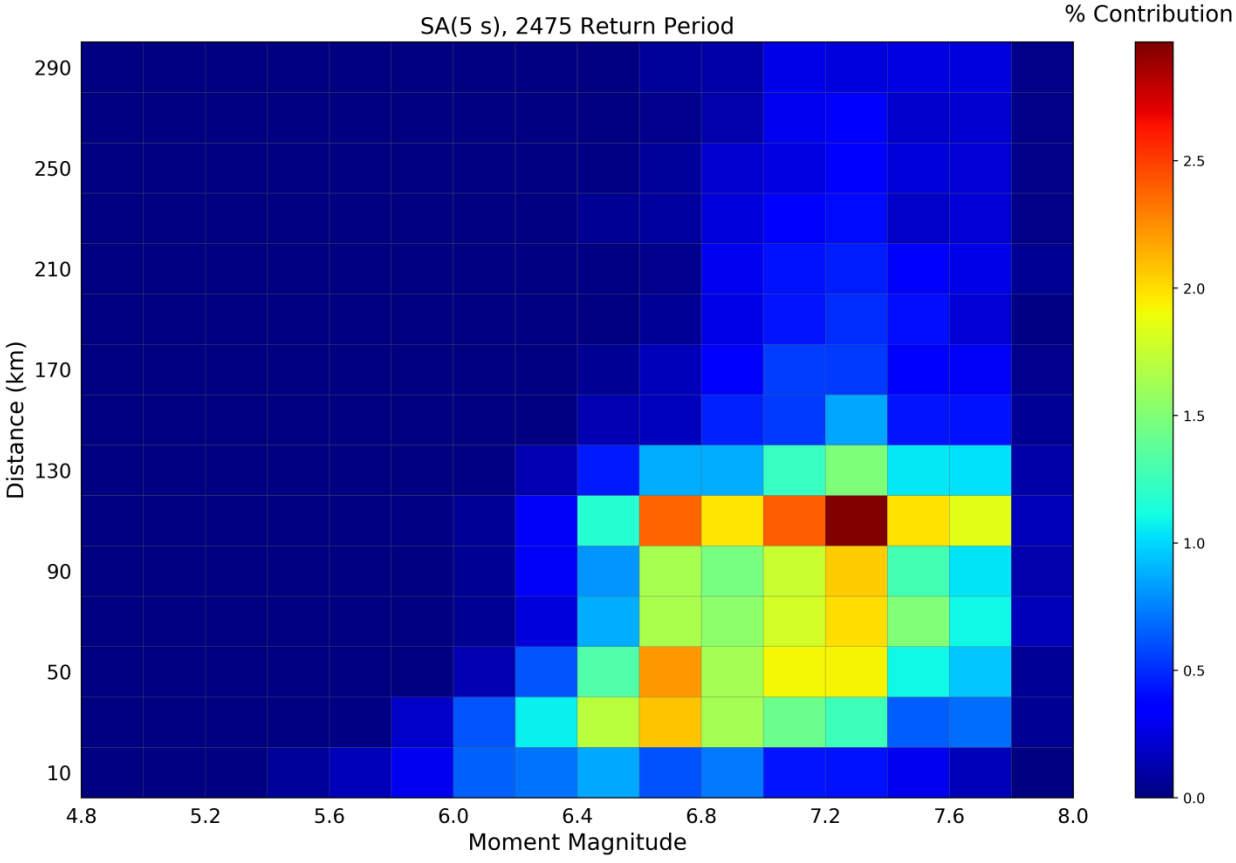
SA(5 s), 2475 Return Period
% Contribution
Distance (km)
290
250
210
170
130
90
50
10
4.8
5.2
5.6
6.0
6.4
6.8
7.2
7.6
8.0
Moment Magnitude
2.5
2.0
1.5
1.0
0.5
0.0